Journal Title
XX(X):1–36

DOI: 10.1177/ToBeAssigned
www.sagepub.com/
SAGE

Supplementary Material for Nonparametric Hyperrectangular Tolerance and Prediction Regions for Setting Multivariate Reference Regions in Laboratory Medicine

Derek S. Young[1] and Thomas Mathew[2]

This document provides supplementary material for the main text. Here we present details about depth functions, results from the coverage study, additional tables and scatterplots for the kidney function example, and additional scatterplots for the IGF reference regions example.

1 Parametric or Nonparametric Reference Regions?

Both parametric and nonparametric approaches have been recommended in the clinical laboratory literature for computing ellipsoidal reference regions. The parametric approach is developed under the assumption of normality, with the understanding that transformation to normality is possible when normality does not hold for the original data. If such a transformation is not possible, a nonparametric approach is recommended[1]. However, transforming the data could alter the multivariate interpretation of test profiles[2]. In view of this, it is certainly desirable to have nonparametric multivariate reference regions that do not rely on the multivariate normality assumption. This is one of the motivations for our work to focus on a nonparametric approach for deriving multivariate reference regions.

[1]Dr. Bing Zhang Department of Statistics, University of Kentucky, Lexington, Kentucky, USA
[2]Department of Mathematics and Statistics, University of Maryland Baltimore County, Baltimore, Maryland, USA

Corresponding author:
Derek S. Young, University of Kentucky, 323 Multidisciplinary Science Building, Lexington, KY, 40536, USA.
Email: derek.young@uky.edu

Prepared using sagej.cls *[Version: 2017/01/17 v1.20]*

1.1 Nonparametric Tolerance Limits and Intervals

For continuous univariate populations, nonparametric (P, γ) tolerance limits are based on order statistics, and are obtained as follows. Let $B \sim \text{Binomial}(n, P)$, and suppose that k is the smallest integer satisfying $\Pr\{B \leq k-1\} \geq \gamma$. In a sample of size n, the kth and $(n-k+1)$th order statistics are, respectively, (P, γ) lower and upper tolerance limits. For the same k, if we write $k = s - r$, for $r < s$, then the rth and sth order statistics form a two-sided (P, γ) tolerance interval. Once the content P and confidence limit γ are specified, a minimum sample size is necessary for the existence of such nonparametric tolerance limits. A one-sided (P, γ) tolerance limit, lower or upper, exists only if $n \geq \ln(1-\gamma)/\ln(P)$. For the existence of a nonparametric two-sided tolerance interval, n must satisfy $(n-1)P^n - nP^{n-1} + 1 \geq \gamma$; we refer to Chapter 8 of Krishnamoorthy and Mathew[3] for details.

1.2 Ellipsoidal vs. Rectangular Regions

In spite of the fact that an ellipsoidal reference region is easy to compute, it should be noted that an ellipsoidal region cannot detect coordinate-wise extremeness; i.e., an ellipsoidal region cannot be used to assess if a particular component of a vector of measurements is extreme. Here is a simple example to illustrate this point. Suppose a reference region in two dimensions is the interior of the circle $(x-5)^2 + (y-5)^2 = 4.5$. Now the point $(7, 6)$ is outside the circle. On the other hand, the point $(7, 5)$ is inside the circle, and so is the point $(5, 6)$. The point $(7, 6)$ being outside the circle, begs the question as to which coordinate is extreme? If we conclude that an x-value of 7 is extreme, how do we reconcile with the conclusion that the point $(7, 5)$ is inside the circle? Similarly, if we conclude that a y-value of 6 is extreme, how do we reconcile with the observation that the point $(5, 6)$ is inside the circle? In other words, such a difficulty cannot be resolved unless we have a way of deciding coordinate-wise extremeness; that is, unless we have a rectangular region.

2 Componentwise Prediction Intervals and Tolerance Intervals Ignoring Correlations: A Coverage Study

We shall present the results from a small simulation study to assess the overall coverage probability when several univariate 95% prediction intervals and $(0.95, 0.95)$ tolerance intervals are used, ignoring the correlations. It is to be expected that this will result in coverage probabilities below 95%, thereby increasing the false positive rates. The simulation study that we have carried out is in the context of the application discussed in the paper on the assessment of kidney function based on reference intervals for three analytes: urine albumin-to-creatinine ratio (UCR), uric acid (UA), and serum creatinine (SC); a detailed data analysis is presented in the paper. Here, data are available for both males and females. The male data consists of a sample of 2529 observations, and the sample correlation matrix is $\begin{pmatrix} 1.000 & -0.009 & -0.025 \\ -0.009 & 1.000 & 0.368 \\ -0.025 & 0.368 & 1.000 \end{pmatrix}$. Assuming multivariate normality to generate the data — using the sample mean vector and sample covariance matrix to be the values of the corresponding parameters — we computed univariate nonparametric 95% prediction intervals for the three analytes; a one-sided upper prediction limit for UACR and two-sided prediction intervals for UA and SC. Based on 10,000 simulated datasets, the simulated coverage probability of the resulting joint prediction region was only

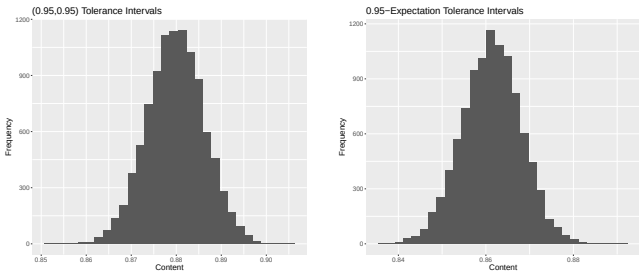

(a) (b)

Figure 1. Content levels for the simulated coverage probability of the kidney function data for (a) joint $(0.95, 0.95)$ nonparametric tolerance intervals and (b) joint 0.95-expectation tolerance intervals.

0.861, well below the nominal level of 0.95. We repeated the simulation using the correlation structure given by $\begin{pmatrix} 1.000 & -0.500 & 0.600 \\ -0.500 & 1.000 & -0.900 \\ 0.600 & -0.900 & 1.000 \end{pmatrix}$, which resulted in a coverage probability of 0.858. We also investigated the performance of univariate nonparametric tolerance intervals having content and confidence level both equal to 0.95; i.e., a $(0.95, 0.95)$ tolerance interval. Such tolerance intervals are based on order statistics. For the joint tolerance region for the three analytes, the content level that meets the 95% confidence level requirement turned out to be 0.880 and 0.906, respectively, for the correlation structures given above. Histograms of the content levels for these simulations are given below.

This limited simulation study highlights what has already been noted by researchers in laboratory medicine, namely, the consequence of ignoring the correlation while computing reference intervals is an increased false positive rate.

3 Definitions of Depth Functions

In this section, we utilize the same notation established in Sections 2 and 3 of the main text.

Liu[4] introduced and discussed four desirable properties of an "ideal" depth function, which Zuo and Serfling[5] later codified into a definition. We follow the latter with presenting the following definition:

Definition 1. Let the mapping $D : \mathbb{R}^p \times \mathcal{F} \to \mathbb{R}$ be bounded and nonnegative. $D_F(\cdot)$ is called a statistical depth function if the following four properties are met:

1. *(Affine invariance.)* $D_{F_{\mathbf{AX}+\mathbf{b}}}(\mathbf{Ax} + \mathbf{b}) = D_{F_{\mathbf{X}}}(\mathbf{x})$ holds for any random vector $\mathbf{X} \in \mathbb{R}^p$, any $p \times p$ nonsingular matrix $\mathbf{A}$, and any $\mathbf{b} \in \mathbb{R}^p$.
2. *(Maximality at center.)* $D_F(\boldsymbol{\vartheta}) = \sup_{\mathbf{x} \in \mathbb{R}^p} D_F(\mathbf{x})$ holds for any $F \in \mathcal{F}$ having center $\boldsymbol{\vartheta}$.
3. *(Monotonicity relative to deepest point.)* For any $F \in \mathcal{F}$ having deepest point $\boldsymbol{\vartheta}$, $D_F(\mathbf{x}) \leq D_F(\boldsymbol{\vartheta} + \rho(\mathbf{x} - \boldsymbol{\vartheta}))$ holds for $\rho \in [0, 1]$.
4. *(Vanishing at infinity.)* $D_F(\mathbf{x}) \to 0$ as $\|\mathbf{x}\| \to \infty$ for each $F \in \mathcal{F}$.

The above are often considered the desirable properties of a depth function, but more extensive lists of properties are occasionally used[6]. Note that in Property 4, as well as throughout our discussion, $\|\cdot\|$ stands for the Euclidean norm.

There are numerous depth functions in the literature, but not all of them are "ideal" according to the properties listed above. For example, some depth functions are not affine invariant, but possess a different property like orthogonal invariance. Fortunately, relaxing the definition of an "ideal" depth function is not detrimental for our purposes, but instead provides a broader class of depth functions for our investigation. In particular, some have a more practical order of computation, thus facilitating more efficient computation of our proposed tolerance regions. Moreover, most existing depth functions can be classified according to their general structure[5,6], which can help when investigating a more computationally advantageous depth function.

Many sample depth functions, including some that we present, are V-statistics or U-statistics. For some of the depth functions, it is helpful to define $\mathcal{B} = \{\mathbf{u} \in \mathbb{R}^p : \|\mathbf{u}\| < 1\}$ and $\mathcal{U} = \{\mathbf{u} \in \mathbb{R}^p : \|\mathbf{u}\| = 1\}$, which are the open unit (hyper)ball and unit (hyper)sphere, respectively. We now define the nine depth functions and their sample versions that comprise our coverage study in the main text:

1. *Simplicial depth*[4]:

$$SD_F(\mathbf{x}) \equiv \Pr_F\left\{\mathbf{x} \in s[\mathbf{X}_1, \ldots, \mathbf{X}_{p+1}]\right\} \quad \text{and} \tag{1}$$

$$SD_{F_n}(\mathbf{x}) = \binom{n}{p+1}^{-1} \sum_{1 \le i_1 < \ldots < i_{p+1} \le n} \mathtt{I}\{\mathbf{x} \in s[\mathbf{X}_{i_1}, \ldots, \mathbf{X}_{i_{p+1}}]\}, \tag{2}$$

   where $s[\mathbf{X}_1, \ldots, \mathbf{X}_{p+1}]$ is the p-dimensional closed simplex with vertices $\mathbf{X}_1, \ldots, \mathbf{X}_{p+1}$ and $\mathtt{I}(\cdot)$ is the indicator function.
2. *Mahalanobis depth*[7]:

$$MD_F(\mathbf{x}; \boldsymbol{\mu}, \boldsymbol{\Sigma}) \equiv \left[1 + \left\|\boldsymbol{\Sigma}^{-1/2}(\mathbf{x} - \boldsymbol{\mu})\right\|^2\right]^{-1} \quad \text{and} \tag{3}$$

$$MD_{F_n}(\mathbf{x}; \bar{\mathbf{x}}, \mathbf{S}) = \left[1 + \left\|\mathbf{S}^{-1/2}(\mathbf{x} - \bar{\mathbf{x}})\right\|^2\right]^{-1}, \tag{4}$$

   where $\boldsymbol{\mu}$ and $\boldsymbol{\Sigma}$ are the mean vector and dispersion matrix under F, respectively, and $\bar{\mathbf{x}}$ and $\mathbf{S}$ are the sample versions.
3. *Tukey depth*[8,9]:

$$TD_F(\mathbf{x}) \equiv \inf_{\mathcal{H}} \{F(\mathcal{H}) : \mathcal{H} \text{ is a closed half-space in } \mathbb{R}^p \text{ containing } \mathbf{x}\} \quad \text{and} \tag{5}$$

$$TD_{F_n}(\mathbf{x}) = \frac{1}{n} \min_{\mathbf{u} \in \mathcal{U}} \sum_{i=1}^{n} \mathtt{I}\{\mathbf{u}^{\mathrm{T}}(\mathbf{X}_i - \mathbf{x}) \ge 0\}. \tag{6}$$

4. *Oja depth*[10]:

$$OD_F(\mathbf{x}) \equiv \left[1 + \mathrm{E}_F\left[\mathrm{Vol}\left\{s[\mathbf{x}, \mathbf{X}_1, \ldots, \mathbf{X}_p]\right\}\right]\right]^{-1} \quad \text{and} \tag{7}$$

$$OD_{F_n}(\mathbf{x}) = \binom{n}{p}^{-1} \left[1 + \sum_{1 \le i_1 < \ldots < i_p \le n} \mathrm{Vol}\left\{s[\mathbf{x}, \mathbf{X}_{i_1}, \ldots, \mathbf{X}_{i_p}]\right\}\right]^{-1}, \tag{8}$$

where $\mathrm{Vol}\{\mathcal{A}\}$ is the volume of the closed set $\mathcal{A}$.

5. *Spatial depth*[11,12]:

$$SptD_F(\mathbf{x}) \equiv 1 - \|Q_F^{-1}(\mathbf{x})\| \quad \text{and} \tag{9}$$

$$SptD_{F_n}(\mathbf{x}) = 1 - \|Q_{F_n}^{-1}(\mathbf{x})\|, \tag{10}$$

where for each $\mathbf{u} \in \mathcal{B}$, the spatial quantile $Q_F(\mathbf{u})$[13] is the solution $\mathbf{x} = \mathbf{x}_\mathbf{u}$ of $-\mathrm{E}\left\{(\mathbf{X} - \mathbf{x})/(\|\mathbf{X} - \mathbf{x}\|)\right\} = \mathbf{u}$.

6. *Zonoid depth*[14,15]:

$$ZD_F(\mathbf{x}) \equiv \max\{\alpha : \mathbf{x} \in Z_\alpha(F)\} \quad \text{and} \tag{11}$$

$$ZD_{F_n}(\mathbf{x}) = \max\{\alpha : \mathbf{x} \in Z_\alpha(F_n)\}, \tag{12}$$

where

$$Z_\alpha(F) = \left\{\int_{\mathbb{R}^p} \mathbf{z} g(\mathbf{z}) dF(\mathbf{z}) : g \in [0, \alpha^{-1}], \int_{\mathbb{R}^p} g(\mathbf{z}) dF(\mathbf{z}) = 1\right\} \quad \text{and}$$

$$Z_\alpha(F_n) = \left\{\sum_{i=1}^n \lambda_i \mathbf{X}_i : \lambda_i \in [0, \alpha^{-1}], \sum_{i=1}^n \lambda_i = 1 \text{ for all } i\right\}$$

are called the *zonoid regions* of F and F_n, respectively. Note that the latter region has range from the mean to the convex hull of the data.

7. *Projection depth*[5]:

$$PD_F(\mathbf{x}) \equiv \left\{1 + \sup_{\mathbf{u} \in \mathcal{U}} \left|\frac{\mathbf{u}^\mathrm{T}\mathbf{x} - \mu(\mathbf{u}^\mathrm{T}\mathbf{X})}{\sigma(\mathbf{u}^\mathrm{T}\mathbf{X})}\right|\right\}^{-1} \quad \text{and} \tag{13}$$

$$PD_{F_n}(\mathbf{x}) = \left\{1 + \sup_{\mathbf{u} \in \mathcal{U}} \left|\frac{\mathbf{u}^\mathrm{T}\mathbf{x} - \mathrm{Med}(\mathbf{u}^\mathrm{T}\mathbf{X}_1, \ldots, \mathbf{u}^\mathrm{T}\mathbf{X}_n)}{\mathrm{MAD}(\mathbf{u}^\mathrm{T}\mathbf{X}_1, \ldots, \mathbf{u}^\mathrm{T}\mathbf{X}_n)}\right|\right\}^{-1}, \tag{14}$$

where $\mu(\mathbf{u}^\mathrm{T}\mathbf{X})$ and $\sigma(\mathbf{u}^\mathrm{T}\mathbf{X})$ are univariate location and scale statistics, respectively, of $\mathbf{u}^\mathrm{T}\mathbf{X}$. Different choices for $\mu(\cdot)$ and $\sigma(\cdot)$ can affect the robustness and efficiency of the estimators[16], so commonly-used robust choices are the median (Med) and the median absolute deviation (MAD), as reflected in (14).

8. *Elliptical depth*[17]:

$$ED_F(\mathbf{x}; \boldsymbol{\Sigma}) \equiv \mathrm{Pr}_F\left\{\mathbf{x} \in B_\boldsymbol{\Sigma}(\mathbf{X}_1, \mathbf{X}_2)\right\} \quad \text{and} \tag{15}$$

$$ED_{F_n}(\mathbf{x}; \mathbf{S}) = \binom{n}{2}^{-1} \sum_{1 \le i_1 < i_2 \le n} \mathrm{I}\left\{\mathbf{x} \in B_\mathbf{S}(\mathbf{X}_{i_1}, \mathbf{X}_{i_2})\right\}, \tag{16}$$

where $B_{\mathbf{\Sigma}}(\mathbf{U},\mathbf{V}) = \{\mathbf{t} : (\mathbf{U}-\mathbf{t})^{\mathrm{T}}\mathbf{\Sigma}^{-1}(\mathbf{V}-\mathbf{t}) \leq 0\}$ is the unique closed hyperellipse formed by $\mathbf{U}$ and $\mathbf{V}$.

9. *Spherical depth*:

$$SpD_F(\mathbf{x}) \equiv \Pr_F\left\{\mathbf{x} \in B_{\mathbf{I}_p}(\mathbf{X}_1,\mathbf{X}_2)\right\} \quad \text{and} \tag{17}$$

$$SpD_{F_n}(\mathbf{x}) = \binom{n}{2}^{-1} \sum_{1\leq i_1<i_2\leq n} \mathtt{I}\left\{\mathbf{x} \in B_{\mathbf{I}_p}(\mathbf{X}_{i_1},\mathbf{X}_{i_2})\right\}, \tag{18}$$

which is the special case of the elliptical depth where $\mathbf{\Sigma} = \mathbf{I}_p$, the $p \times p$ identity matrix.

Note that the Mahalanobis depth and elliptical depth each depend on the dispersion matrix $\mathbf{\Sigma}$. For our purposes, we use the sample variance-covariance matrix $\mathbf{S}$ when computing depth values. One could explore the use of other scatter matrices, such as the M-estimator of scatter[18]. However, the use of such alternative matrices is beyond the scope of our discussion.

4 Additional Practical Consideration of Depth Functions

Our choice of depth functions was guided by a couple of practical considerations. As noted in Serfling et al.[6], the feasibility of computing data depth is a function of the size n and dimension p of the data, with severe practical limitations arising in the case of higher p. The simplicial, Tukey, Mahalanobis, and Oja depths are all well-studied in the literature and, thus, illustrative to use in our procedure. However, computational limitations arise with, for example, simplicial and Oja depth, which have order of computation $\mathcal{O}(n^{p+1})$ and $\mathcal{O}(n^p)$, respectively. Some algorithms have been developed that improve the order of computation for certain depth functions and settings[19,20]. But for the larger n, higher p settings, we suggest using the elliptical and spherical depths[17], which have order of computation $\mathcal{O}(pn^2)$. Regardless, the algorithm we present for constructing multivariate hyperrectangular tolerance regions can accommodate any depth function.

Another practical consideration is that the depth functions we use are all available in various `R`[21] packages. The elliptical and spherical depths can be calculated using the `depth` function in the `mixtools` package[22], while all other depth functions can be calculated using the `ddalpha` package[23]. For some of the more computationally-demanding depth functions, the `ddalpha` package optionally allows for calculating highly-accurate approximations using novel algorithms[16,24]. Where applicable, we utilize these approximations due to the large number of conditions in our simulation study.

The practical considerations we highlighted above and in the main text concern the computational resources available for performing the depth calculations. However, a practical concern addressed in the literature is the dependency on the depth function when using them in nonparametric testing or nonparametric descriptions of data. For example, Dovoedo and Chakraborti[25] illustrated the differences in power for depth-based tests of location in multivariate skewed distributions when using different depth functions. Dang and Serfling[26] investigated the choice of depth function in the context of multivariate outlier identification and masking properties. Their results show favorable performance with the Mahalanobis depth and projection depth. Serfling and Wijesuriya[27] addressed depth-based approaches for describing and visualizing functional data, where they recommended the use of spatial depth as it provides an "appealing combination of robustness, efficiency, computational ease, and versatility."

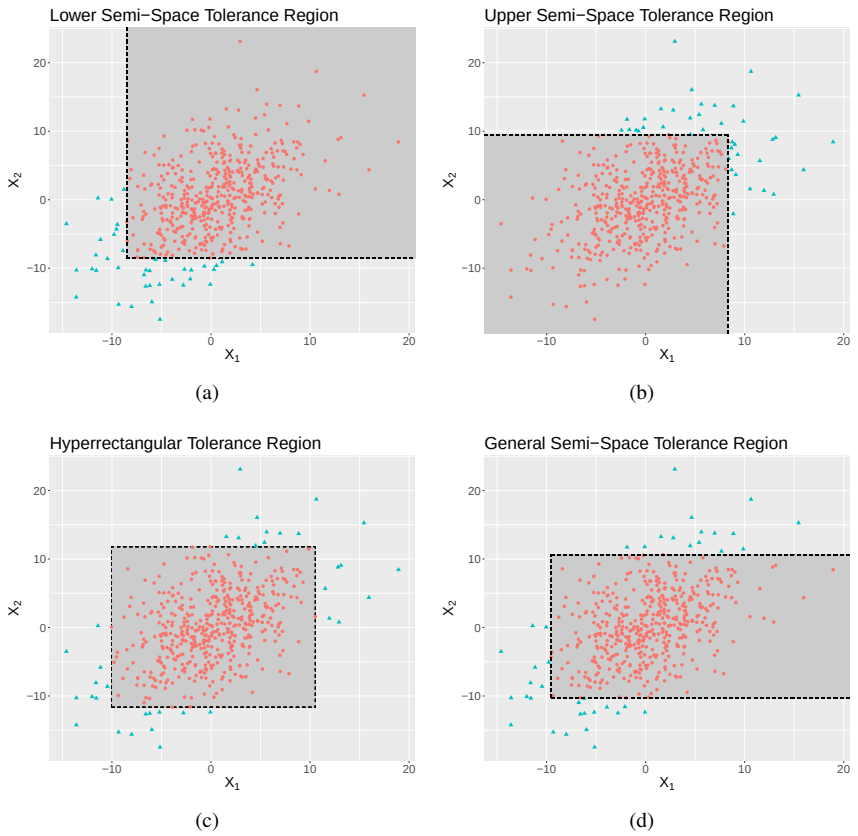

Figure 2. Examples of (a) lower semi-space, (b) upper semi-space, (c) hyperrectangular, and (d) general semi-space tolerance regions for the bivariate setting.

5 Illustration of Different Regions Calculated Using Proposed Algorithm

Figure 2 illustrates the different regions calculated using our algorithm for the case of $p = 2$. In each figure, the calculated rectangular region is shaded and points that are trimmed are plotted as triangles. Figures 2(a), 2(b), and 2(c) illustrate lower semi-space, upper semi-space, and hyperrectangular tolerance regions, respectively. We note that, if so desired, the sets given in the main text can be modified to have a combination of lower limits, upper limits, and two-sided intervals across the dimensions of $\mathbf{X}$. For example, Figure 2(d) is such a region with a lower limit for the first dimension and a two-sided interval for the second dimension. We did not include a definition for such a general semi-space tolerance region in order to simplify the notation used, however, all facets of our remaining discussion are applicable to such settings.

6 The Multivariate Regression Setting

Suppose that we now have p-dimensional vectors $\mathbf{y}_1, \ldots, \mathbf{y}_n$ that depend on q-dimensional covariate vectors $\mathbf{x}_1, \ldots, \mathbf{x}_n$. We can construct hyperrectangular tolerance regions for the multivariate linear regression model, where for subject i, $\mathbf{y}_i = \mathbf{B}\mathbf{x}_i + \boldsymbol{\epsilon}_i$. In this model, $\mathbf{B}$ is a $p \times q$ matrix of regression parameters, and the $\boldsymbol{\epsilon}_i$ are random error vectors. Note that, by convention, we assume the first entry in $\mathbf{x}_i$ is 1 to accommodate an intercept term.

Let $\hat{\mathbf{B}}$ be an estimate (e.g., the ordinary least squares estimate) of $\mathbf{B}$ and $\hat{\mathbf{y}}_i = \hat{\mathbf{B}}\mathbf{x}_i$ the fitted value of the response vector. We can apply our algorithm to the residual vectors $\mathbf{r}_i = \mathbf{y}_i - \hat{\mathbf{y}}_i$, $i = 1, \ldots, n$, and then add the nonparametric limits to $\hat{\mathbf{y}}_h = \hat{\mathbf{B}}\mathbf{x}_h$ for any given (possibly new) covariate vector $\mathbf{x}_h$. Again, this procedure can be used to obtain either (P, γ) or β-expectation tolerance regions.

7 Lucky (p, n, γ, P) Phenomenon

While we achieved results close to the nominal level in our simulations, there is the possibility that particular combinations of n, p, γ, and P could yield more spurious conservative results. For example, Figure 3 shows simulated coverage probabilities of nonparametric $(0.95, 0.95)$ hyperrectangular tolerance regions based on our algorithm. We considered bivariate and trivariate standard normal distributions for the simulations, and sample sizes of $n \in \{300, \ldots, 500\}$. Similar oscillatory behavior is demonstrated and discussed for univariate nonparametric tolerance intervals[28]. The range of coverage probabilities are a bit tighter for the trivariate setting ($p = 3$) in Figure 3(a) when compared to the bivariate setting ($p = 2$) in Figure 3(b), which further highlights the effect of the dimension p on the coverage probabilities. In the spirit of Brown, Cai, and DasGupta[29] who refer to the "lucky (p, n) phenomenon" as when near nominal coverage probabilities are achieved for certain (p, n) pairs in constructing confidence intervals for p in a $Bin(n, p)$ distribution, we could state for our nonparametric setting that we have a "lucky (p, n, γ, P) phenomenon." Note that Figure 3 is a simulation-based assessment of the coverage probabilities of nonparametric $(0.95, 0.95)$ hyperrectangular tolerance regions, so our results are reflecting some variability due to the random samples generated. However, the general oscillatory behavior and the strong indication that most settings depicted are meeting the nominal level, suggests that our procedure could be behaving similar to those confidence interval procedures that Brown, Cai, and DasGupta[29] refer to as having "lucky (p, n) pairs."

8 Bonferroni Correction

When multiple analytical measurements are obtained from specimens on the same patient, computing separate univariate reference intervals by applying a Bonferroni correction on each analyte could result in univariate intervals that are too wide, leading to high numbers of false normal results. This should be clear from the coverage probabilities and expected volumes reported in the main text, and from the additional numerical results reported in the next section. Here we shall give some details of the Bonferroni correction, and also some hyperrectangular tolerance intervals based on datasets generated from a trivariate normal distributions.

If one calculates individual tolerance intervals and applies a Bonferroni correction, then the correction is applied to the confidence level for the individual β-expectation tolerance intervals, and to the confidence and content levels for the individual (P, γ) tolerance intervals. Specifically, letting

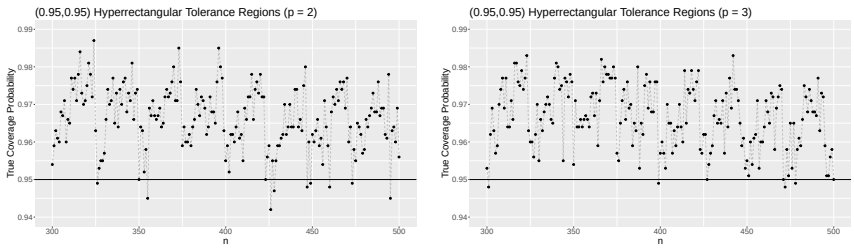

(a) (b)

Figure 3. Simulated coverage probabilities of nonparametric $(0.95, 0.95)$ hyperrectangular tolerance regions for (a) the bivariate standard normal and (b) the trivariate standard normal. The Mahalanobis depth was used in the algorithm for constructing the hyperrectangular regions.

$g_p(z) = 1 - (1 - z)/p$, Bonferroni-corrected (P, γ) hyperrectangular tolerance regions are based on $(g_p(P), g_p(\gamma))$ tolerance intervals, where recall that p is the dimension of the data. A derivation of $g_p(z)$ is given below.

Let $\mathbf{X} = (X_1, \ldots, X_p)^{\mathsf{T}} \sim F$, and suppose that we are interested in calculating a nonparametric (P, γ) hyperrectangular tolerance region using Bonferroni-corrected nonparametric tolerance intervals. For this discussion, assume that we are constructing one-sided upper tolerance intervals for each dimension of $\mathbf{X}$. The following argument is analogous for one-sided lower tolerance intervals, two-sided tolerance intervals, or any combination of such intervals. Define the events $A_i = \{X_i \leq U_i\}$, $i = 1, \ldots, p$, where U_i is the desired upper tolerance limit for that dimension. The A_i are random because U_i is based on the data, so the criterion for the (P, γ) tolerance region is

$$\Pr\left\{\Pr\left(\bigcap_{i=1}^{p} A_i\right) \geq P\right\} = \gamma. \tag{19}$$

The Bonferroni correction applied to the inner probability statement in the above yields the following bound:

$$\Pr\left\{\bigcap_{i=1}^{p} A_i\right\} \geq 1 - \sum_{i=1}^{p} \Pr\left\{A_i^C\right\}. \tag{20}$$

To ensure that the inner probability criterion in (19) is met, set $1 - \sum_{i=1}^{p} \Pr\left\{A_i^C\right\} = P$, which implies that

$$\Pr(A_i) = 1 - \frac{1 - P}{p}, \quad \text{for each } i.$$

Using the right-hand side as an above limit for the $\Pr(A_i)$, define the events

$$B_i = \left\{\Pr(A_i) = 1 - \frac{1 - P}{p}\right\},$$

$i = 1, \ldots, p$. Again, the B_i are random. An analogous application of the Bonferroni correction to $\Pr\{\bigcap_{i=1}^{p} B_i\}$ yields the same bound as in (20) but in terms of the B_i. Thus, to ensure the criterion in (19) is met, set $1 - \sum_{i=1}^{p} \Pr\left\{B_i^C\right\} = \gamma$, which implies that

$$\Pr(B_i) = 1 - \frac{1-\gamma}{p}, \quad \text{for each } i.$$

Thus, the Bonferroni correction $g_p(z) = 1 - (1-z)/p$ has been applied to both P and γ. Note that this is the standard correction applied to β for the β-expectation tolerance regions when using individual Bonferroni-corrected intervals.

In addition to the numerical results on the coverage probabilities and expected volumes reported in the main text and in this Supplementary Material, we shall also highlight the conservative behavior of the Bonferroni correction by computing the hyperrectangular tolerance regions based on datasets generated from a trivariate normal distribution with mean vector zero, variances all equal to one, and having a common correlation ρ assuming two values: $\rho = 0$ and $\rho = 0.95$. Under each case, we generated a sample of $n = 1000$ observations. Table 1 shows the resulting hyperrectangular regions when using the Bonferroni correction, using the bounding region of the multivariate normal tolerance ellipse, the bounding region of the convex hull based on spherical depth, and our approach with elliptical depth. Clearly the Bonferroni-corrected tolerance intervals are wider than those determined by our algorithm in all settings, especially in the highly-correlated setting. The normal-based approach is slightly narrower (i.e., liberal) in the uncorrelated setting, but slightly wider (i.e., conservative) in the highly-correlated setting. This is consistent with the simulation results presented in the main text. Moreover, the bounding region of the convex hull based on spherical depth is always the widest, which again is consistent with the conservative results we obtained in the main text when developing the tolerance region in this manner.

9 Additional Results for Coverage Study

Let $\mathcal{N}_p(\boldsymbol{\mu}, \Sigma)$ denote the p-dimensional multivariate normal distribution with mean vector $\boldsymbol{\mu}$ and variance-covariance matrix Σ, $\mathcal{E}_p(\boldsymbol{\lambda})$ denote the p-dimensional (uncorrelated) multivariate exponential distribution with rate vector $\boldsymbol{\lambda}$, $t_p(\nu, \Sigma)$ denote the p-dimensional multivariate t-distribution with ν degrees of freedom and scale matrix Σ, and $\mathcal{C}_p(\Sigma)$ denote the p-dimensional multivariate Cauchy distribution with scale matrix Σ. We assessed the robustness of our hyperrectangular tolerance region procedure by generating data from the following seven distributions: (1) $\mathcal{N}_2\left(\mathbf{0}_2, \begin{pmatrix} 1 & 0.5 \\ 0.5 & 1 \end{pmatrix}\right)$, (2) $\mathcal{E}_2\left(\begin{pmatrix} 1 \\ 0.5 \end{pmatrix}\right)$, (3) $t_2\left(4, \begin{pmatrix} 1 & 0.5 \\ 0.5 & 1 \end{pmatrix}\right)$, (4) $\mathcal{N}_3\left(\mathbf{0}_3, \mathbf{I}_3\right)$, (5) $\mathcal{N}_3\left(\mathbf{0}_3, \begin{pmatrix} 1 & 0.8 & 0.6 \\ 0.8 & 1 & 0.6 \\ 0.6 & 0.6 & 1 \end{pmatrix}\right)$, (6) $t_3\left(5, \mathbf{I}_3\right)$, and (7) $\mathcal{C}_3\left(\mathbf{I}_3\right)$. Note that $\mathbf{0}_p$ is the p-dimensional vector of all zeroes.

Tables 2 – 9 report the coverage probabilities and expected volumes under all of the simulation conditions we considered. Each table is structured such that the top-half corresponds to the (P, γ) tolerance region approach and the bottom-half corresponds to the β-expectation tolerance region approach. Starting with the third column of each table, the results are given, respectively, for the following methods: simplicial depth (Simp), Mahalanobis depth (Mah), Tukey depth (Tukey), Oja depth (Oja), spatial depth (Spat), zonoid depth (Zon), projection depth (Proj), elliptical depth (Ellip), spherical depth

Table 1. Tolerance regions based on the Bonferroni correction, using the bounding region of the multivariate normal tolerance ellipse, the bounding region of the convex hull based on spherical depth, and our appoach. These are applied to two simulated trivariate normal datasets of size $n = 1000$. The top-half of the table are results for the $(0.90, 0.95)$ tolerance regions. The bottom-half of the table are results for the 0.95-expectation tolerance regions.

ρ	$\mathbf{X}$	$(0.90, 0.95)$ Tolerance Region			
		Bonferroni	Normal	Li-Liu	Our Algorithm
0	X_1	$(-2.31, 2.14)$	$(-1.60, 1.55)$	$(-3.73, 2.85)$	$(-2.30, 2.08)$
	X_2	$(-2.17, 2.25)$	$(-1.90, 1.84)$	$(-2.67, 2.73)$	$(-2.19, 2.02)$
	X_3	$(-2.31, 2.19)$	$(-1.82, 1.83)$	$(-2.66, 2.58)$	$(-2.23, 2.19)$
0.95	X_1	$(-2.40, 2.28)$	$(-2.43, 2.50)$	$(-4.28, 2.67)$	$(-1.98, 1.99)$
	X_2	$(-2.42, 2.29)$	$(-2.44, 2.46)$	$(-3.90, 2.64)$	$(-1.92, 1.97)$
	X_3	$(-2.43, 2.17)$	$(-2.43, 2.47)$	$(-3.99, 2.76)$	$(-1.97, 2.01)$
ρ	$\mathbf{X}$	0.95-Expectation Tolerance Region			
		Bonferroni	Normal	Li-Liu	Our Algorithm
0	X_1	$(-2.62, 2.18)$	$(-1.82, 1.77)$	$(-3.73, 2.85)$	$(-2.30, 2.14)$
	X_2	$(-2.27, 2.43)$	$(-2.17, 2.11)$	$(-2.67, 2.73)$	$(-2.37, 2.19)$
	X_3	$(-2.65, 2.22)$	$(-2.09, 2.10)$	$(-2.92, 2.72)$	$(-2.33, 2.42)$
0.95	X_1	$(-2.50, 2.40)$	$(-2.79, 2.86)$	$(-4.28, 2.67)$	$(-2.11, 2.23)$
	X_2	$(-2.78, 2.31)$	$(-2.80, 2.82)$	$(-3.90, 2.64)$	$(-2.07, 2.19)$
	X_3	$(-2.61, 2.18)$	$(-2.78, 2.82)$	$(-3.99, 2.76)$	$(-2.12, 2.17)$

(Spher), classic nonparametric tolerance intervals with a Bonferroni correction (Bonf), constructing a bounding hyperrectangular region of the convex hull constructed using spherical depth (CHull), and constructing a bounding hyperrectangular region of the normal-based tolerance region. Note that in the tables where we report the expected volumes, we use $a^b \equiv a \times 10^b$ as short-hand for scientific notation. An overall assessment of these simulation results is given in the main text.

Table 2. Coverage probabilities of $(0.90, 0.95)$ hyperrectangular tolerance regions (top-half of table) and 0.95-expectation hyperrectangular tolerance regions (bottom-half of table).

$(0.90, 0.95)$ **Hyperrectangular Tolerance Regions**													
Distribution	n	**Simp**	**Mah**	**Tukey**	**Oja**	**Spat**	**Zon**	**Proj**	**Ellip**	**Spher**	**Bonf**	**CHull**	**Norm**
Bivariate	300	0.967	0.956	0.959	0.971	0.957	0.955	0.964	0.955	0.960	0.998	0.995	0.025
Normal	1000	0.967	0.961	0.969	0.958	0.961	0.960	0.961	0.961	0.957	1.000	1.000	0.003
Bivariate	300	0.970	0.963	0.960	0.984	0.969	0.956	0.963	0.966	0.971	0.998	0.977	0.964
Exponential	1000	0.965	0.957	0.958	0.960	0.958	0.954	0.952	0.955	0.961	1.000	1.000	1.000
Bivariate t	300	0.975	0.965	0.961	0.971	0.964	0.958	0.962	0.960	0.959	1.000	0.982	0.218
	1000	0.968	0.970	0.968	0.968	0.961	0.963	0.968	0.960	0.959	1.000	1.000	0.277
Trivariate	300	0.977	0.963	0.974	0.967	0.964	0.972	0.973	0.964	0.962	1.000	1.000	0.246
Normal($\Sigma = \mathbf{I}_3$)	1000	0.961	0.957	0.961	0.960	0.953	0.962	0.968	0.954	0.958	1.000	1.000	0.321
Trivariate	300	0.984	0.967	0.973	0.970	0.966	0.969	0.975	0.968	0.969	1.000	1.000	0.820
Normal ($\Sigma \neq \mathbf{I}_3$)	1000	0.966	0.956	0.959	0.959	0.955	0.955	0.960	0.955	0.956	1.000	1.000	0.994
Trivariate t	300	0.977	0.965	0.970	0.971	0.962	0.970	0.969	0.964	0.965	1.000	1.000	0.178
	1000	0.967	0.963	0.959	0.969	0.962	0.957	0.964	0.960	0.958	1.000	1.000	0.255
Trivariate	300	0.989	0.977	0.974	0.982	0.980	0.979	0.976	0.979	0.978	1.000	1.000	0.994
Cauchy	1000	0.975	0.966	0.960	0.959	0.964	0.963	0.962	0.963	0.958	1.000	1.000	1.000

0.95-Expectation Hyperrectangular Tolerance Regions													
Distribution	n	**Simp**	**Mah**	**Tukey**	**Oja**	**Spat**	**Zon**	**Proj**	**Ellip**	**Spher**	**Bonf**	**CHull**	**Norm**
Bivariate	300	0.940	0.939	0.939	0.940	0.939	0.938	0.940	0.939	0.939	0.957	0.956	0.936
Normal	1000	0.947	0.947	0.947	0.946	0.946	0.946	0.947	0.946	0.946	0.954	0.972	0.937
Bivariate	300	0.940	0.940	0.939	0.940	0.940	0.938	0.940	0.940	0.940	0.954	0.953	0.980
Exponential	1000	0.947	0.947	0.947	0.947	0.947	0.946	0.947	0.947	0.947	0.951	0.967	0.981
Bivariate t	300	0.940	0.939	0.940	0.940	0.939	0.939	0.940	0.939	0.939	0.960	0.952	0.927
	1000	0.947	0.947	0.947	0.947	0.947	0.947	0.947	0.947	0.947	0.958	0.964	0.930
Trivariate	300	0.934	0.932	0.933	0.932	0.932	0.933	0.933	0.931	0.932	0.952	0.977	0.927
Normal($\Sigma = \mathbf{I}_3$)	1000	0.945	0.944	0.944	0.945	0.944	0.944	0.945	0.944	0.944	0.953	0.990	0.928
Trivariate	300	0.936	0.933	0.934	0.934	0.933	0.934	0.934	0.933	0.932	0.960	0.980	0.964
Normal ($\Sigma \neq \mathbf{I}_3$)	1000	0.946	0.945	0.945	0.945	0.945	0.945	0.945	0.945	0.945	0.962	0.992	0.964
Trivariate t	300	0.936	0.933	0.934	0.933	0.933	0.934	0.934	0.933	0.933	0.957	0.978	0.915
	1000	0.945	0.945	0.945	0.945	0.945	0.944	0.945	0.944	0.945	0.958	0.991	0.915
Trivariate	300	0.939	0.936	0.935	0.935	0.935	0.935	0.935	0.935	0.935	0.969	0.983	0.972
Cauchy	1000	0.946	0.945	0.945	0.945	0.945	0.945	0.945	0.945	0.945	0.972	0.992	0.984

Table 3. Expected volumes of $(0.90, 0.95)$ hyperrectangular tolerance regions (top-half of table) and 0.95-expectation hyperrectangular tolerance regions (bottom-half of table). Here, we use $a^b \equiv a \times 10^b$ as short-hand for scientific notation.

$(0.90, 0.95)$ **Hyperrectangular Tolerance Regions**													
Distribution	n	**Simp**	**Mah**	**Tukey**	**Oja**	**Spat**	**Zon**	**Proj**	**Ellip**	**Spher**	**Bonf**	**CHull**	**Norm**
Bivariate	300	18.02	17.48	17.68	20.26	17.45	17.59	17.61	17.49	17.52	20.46	19.99	12.60
Normal	1000	16.09	15.97	16.01	16.51	15.96	15.97	16.01	15.97	15.97	17.76	19.67	13.14
Bivariate	300	40.49	24.05	33.73	28.36	24.15	35.57	24.17	24.57	25.00	39.39	42.16	27.97
Exponential	1000	37.46	20.27	30.11	20.66	20.31	31.90	20.27	20.39	20.98	32.52	45.65	29.92
Bivariate t	300	38.86	36.37	37.19	43.37	36.47	37.25	36.44	36.73	36.73	51.97	43.82	25.02
	1000	31.41	31.05	31.16	31.99	31.01	31.16	31.07	31.04	31.04	39.54	39.00	26.14
Trivariate	300	109.42	96.28	97.85	96.90	95.92	98.97	97.47	96.10	96.18	134.07	175.08	65.31
Normal($\Sigma = \mathbf{I}_3$)	1000	90.17	84.24	84.65	84.48	84.13	84.61	84.80	84.18	84.28	97.98	220.44	69.09
Trivariate	300	100.01	85.55	86.63	86.14	85.45	87.73	86.33	85.55	85.06	134.84	178.72	76.34
Normal ($\Sigma \neq \mathbf{I}_3$)	1000	77.68	73.49	73.77	73.66	73.41	73.70	73.76	73.42	73.43	98.39	226.93	80.51
Trivariate t	300	382.54	257.95	266.97	259.29	257.98	275.46	260.62	262.65	262.01	543.29	1.04^{03}	139.71
	1000	244.48	204.26	205.63	204.65	204.03	206.10	204.88	204.14	204.23	295.58	1.45^{03}	147.14
Trivariate	300	1.63^{09}	7.68^{04}	5.55^{04}	5.69^{04}	6.00^{04}	9.67^{04}	4.53^{04}	6.40^{04}	6.42^{04}	3.86^{07}	6.27^{13}	1.34^{12}
Cauchy	1000	9.66^{08}	2.63^{04}	1.90^{04}	2.15^{04}	2.56^{04}	2.95^{04}	1.79^{04}	2.40^{04}	1.90^{04}	2.85^{05}	1.33^{15}	5.03^{12}

0.95-Expectation Hyperrectangular Tolerance Regions													
Distribution	n	**Simp**	**Mah**	**Tukey**	**Oja**	**Spat**	**Zon**	**Proj**	**Ellip**	**Spher**	**Bonf**	**CHull**	**Norm**
Bivariate	300	19.25	18.63	18.83	21.31	18.63	18.76	18.75	18.66	18.67	21.59	21.69	18.23
Normal	1000	19.48	19.23	19.33	19.88	19.24	19.27	19.28	19.25	19.24	20.35	24.44	18.07
Bivariate	300	42.39	26.67	36.73	31.12	26.77	38.39	26.77	27.21	27.60	39.45	45.76	46.22
Exponential	1000	48.27	26.99	38.14	27.53	26.99	40.14	27.03	27.16	27.65	38.31	60.36	46.26
Bivariate t	300	43.91	40.59	41.86	47.60	40.75	41.86	40.84	41.29	41.17	57.91	52.29	36.19
	1000	43.89	42.79	43.18	43.89	42.79	43.11	42.79	42.91	42.86	50.48	58.13	35.95
Trivariate	300	111.89	98.82	100.69	99.80	98.50	102.04	100.22	98.65	98.74	120.94	181.18	105.13
Normal($\Sigma = \mathbf{I}_3$)	1000	116.77	105.40	105.96	105.79	105.31	105.93	106.01	105.19	105.23	114.95	242.01	103.68
Trivariate	300	102.25	88.31	89.83	88.92	88.23	90.94	89.16	88.33	88.07	120.66	181.61	123.19
Normal ($\Sigma \neq \mathbf{I}_3$)	1000	104.16	94.50	95.05	94.71	94.41	94.88	94.86	94.43	94.57	115.57	247.31	120.91
Trivariate t	300	398.77	270.26	280.47	271.81	270.65	291.39	272.47	275.83	276.15	450.27	1.07^{03}	230.96
	1000	394.85	299.58	302.47	299.70	299.12	303.67	301.16	299.71	299.60	390.50	1.98^{03}	222.79
Trivariate	300	1.27^{09}	7.30^{04}	6.82^{04}	4.32^{05}	7.48^{04}	9.64^{04}	5.62^{04}	8.98^{04}	7.70^{04}	5.98^{06}	4.57^{13}	1.57^{12}
Cauchy	1000	8.61^{10}	8.84^{04}	7.25^{04}	7.63^{04}	8.78^{04}	1.01^{05}	6.69^{04}	8.30^{04}	7.44^{04}	9.26^{05}	6.15^{12}	8.21^{13}

Table 4. Coverage probabilities of $(0.90, 0.95)$ upper semi-space tolerance regions (top-half of table) and 0.95-expectation upper semi-space tolerance regions (bottom-half of table).

$(0.90, 0.95)$ **Upper Semi-Space Tolerance Regions**													
Distribution	n	**Simp**	**Mah**	**Tukey**	**Oja**	**Spat**	**Zon**	**Proj**	**Ellip**	**Spher**	**Bonf**	**CHull**	**Norm**
Bivariate	300	0.952	0.949	0.952	0.949	0.946	0.953	0.948	0.949	0.952	1.000	1.000	0.984
Normal	1000	0.959	0.959	0.954	0.954	0.960	0.957	0.963	0.958	0.962	1.000	1.000	1.000
Bivariate	300	0.959	0.953	0.951	0.950	0.950	0.953	0.945	0.947	0.939	0.999	1.000	1.000
Exponential	1000	0.956	0.949	0.948	0.947	0.944	0.947	0.947	0.947	0.954	0.998	1.000	1.000
Bivariate t	300	0.949	0.945	0.944	0.950	0.943	0.947	0.942	0.946	0.948	1.000	1.000	0.994
	1000	0.950	0.953	0.944	0.950	0.952	0.951	0.950	0.952	0.951	1.000	1.000	1.000
Trivariate	300	0.969	0.964	0.964	0.961	0.960	0.960	0.966	0.957	0.968	1.000	1.000	0.746
Normal($\Sigma = \mathbf{I}_3$)	1000	0.955	0.954	0.955	0.956	0.953	0.955	0.954	0.954	0.962	1.000	1.000	0.810
Trivariate	300	0.965	0.956	0.954	0.961	0.957	0.959	0.957	0.957	0.955	1.000	1.000	1.000
Normal ($\Sigma \neq \mathbf{I}_3$)	1000	0.963	0.955	0.958	0.958	0.957	0.957	0.958	0.957	0.958	1.000	1.000	1.000
Trivariate t	300	0.950	0.951	0.949	0.950	0.954	0.949	0.954	0.946	0.949	1.000	1.000	0.853
	1000	0.960	0.963	0.960	0.955	0.961	0.956	0.954	0.962	0.961	1.000	1.000	0.926
Trivariate	300	0.957	0.964	0.947	0.953	0.962	0.951	0.953	0.954	0.951	1.000	1.000	1.000
Cauchy	1000	0.948	0.952	0.948	0.947	0.946	0.951	0.948	0.947	0.950	1.000	1.000	1.000

0.95-Expectation Upper Semi-Space Tolerance Regions													
Distribution	n	**Simp**	**Mah**	**Tukey**	**Oja**	**Spat**	**Zon**	**Proj**	**Ellip**	**Spher**	**Bonf**	**CHull**	**Norm**
Bivariate	300	0.948	0.947	0.947	0.948	0.947	0.947	0.948	0.947	0.947	0.958	0.978	0.968
Normal	1000	0.949	0.949	0.949	0.949	0.949	0.949	0.949	0.949	0.949	0.955	0.986	0.969
Bivariate	300	0.947	0.946	0.947	0.947	0.946	0.946	0.946	0.946	0.947	0.954	0.980	0.983
Exponential	1000	0.949	0.949	0.949	0.949	0.949	0.949	0.949	0.949	0.949	0.951	0.990	0.984
Bivariate t	300	0.947	0.947	0.947	0.947	0.947	0.946	0.947	0.947	0.947	0.960	0.976	0.963
	1000	0.949	0.949	0.949	0.949	0.949	0.949	0.949	0.949	0.949	0.958	0.982	0.965
Trivariate	300	0.945	0.944	0.944	0.944	0.944	0.944	0.944	0.944	0.944	0.952	0.989	0.963
Normal($\Sigma = \mathbf{I}_3$)	1000	0.948	0.948	0.948	0.948	0.948	0.948	0.948	0.948	0.948	0.953	0.995	0.963
Trivariate	300	0.944	0.943	0.944	0.944	0.943	0.944	0.944	0.943	0.943	0.962	0.991	0.982
Normal ($\Sigma \neq \mathbf{I}_3$)	1000	0.948	0.948	0.948	0.948	0.948	0.948	0.948	0.948	0.948	0.963	0.996	0.982
Trivariate t	300	0.944	0.942	0.943	0.942	0.942	0.942	0.943	0.942	0.942	0.954	0.989	0.954
	1000	0.948	0.948	0.948	0.948	0.948	0.948	0.948	0.948	0.948	0.956	0.995	0.954
Trivariate	300	0.945	0.944	0.944	0.944	0.944	0.944	0.944	0.943	0.943	0.962	0.990	0.982
Cauchy	1000	0.948	0.948	0.948	0.948	0.948	0.948	0.948	0.948	0.948	0.964	0.995	0.990

Table 5. Expected volumes of $(0.90, 0.95)$ upper semi-space tolerance regions (top-half of table) and 0.95-expectation upper semi-space tolerance regions (bottom-half of table). Here, we use $a^b \equiv a \times 10^b$ as short-hand for scientific notation.

$(0.90, 0.95)$ **Upper Semi-Space Tolerance Regions**													
Distribution	n	**Simp**	**Mah**	**Tukey**	**Oja**	**Spat**	**Zon**	**Proj**	**Ellip**	**Spher**	**Bonf**	**CHull**	**Norm**
Bivariate	300	3.10	3.07	3.08	3.40	3.07	3.07	3.08	3.07	3.07	3.87	5.05	3.16
Normal	1000	2.79	2.78	2.78	2.82	2.78	2.78	2.78	2.78	2.78	3.22	4.93	3.28
Bivariate	300	22.33	22.04	22.15	25.25	22.05	22.08	22.13	22.09	22.32	27.30	42.53	28.17
Exponential	1000	19.89	19.80	19.86	20.16	19.81	19.81	19.82	19.83	20.19	21.99	46.06	30.08
Bivariate t	300	5.31	5.26	5.26	5.92	5.26	5.26	5.25	5.25	5.24	7.82	10.97	6.25
	1000	4.49	4.48	4.48	4.54	4.48	4.48	4.47	4.47	4.48	5.86	9.75	6.53
Trivariate	300	8.68	7.81	7.86	7.85	7.79	7.87	7.86	7.81	7.80	11.64	22.25	8.17
Normal($\Sigma = \mathbf{I}_3$)	1000	6.97	6.86	6.87	6.87	6.86	6.87	6.88	6.86	6.86	8.31	27.74	8.63
Trivariate	300	7.06	6.38	6.40	6.40	6.38	6.41	6.41	6.38	6.35	11.73	22.53	9.63
Normal ($\Sigma \neq \mathbf{I}_3$)	1000	5.51	5.44	5.46	5.45	5.44	5.44	5.47	5.44	5.44	8.32	28.44	10.08
Trivariate t	300	21.30	16.75	16.91	16.84	16.75	16.92	16.87	16.76	16.71	34.42	127.18	17.73
	1000	14.20	13.95	13.97	13.95	13.94	13.97	13.96	13.92	13.92	19.74	176.14	18.70
Trivariate	300	5.98^{05}	1.49^{03}	1.36^{03}	1.45^{03}	1.46^{03}	1.54^{03}	1.29^{03}	1.42^{03}	1.36^{03}	5.98^{04}	3.98^{09}	3.45^{11}
Cauchy	1000	660.18	787.74	631.63	718.57	736.77	749.48	622.65	722.41	629.43	3.68^{03}	6.96^{09}	3.49^{13}

0.95-Expectation Upper Semi-Space Tolerance Regions													
Distribution	n	**Simp**	**Mah**	**Tukey**	**Oja**	**Spat**	**Zon**	**Proj**	**Ellip**	**Spher**	**Bonf**	**CHull**	**Norm**
Bivariate	300	3.70	3.66	3.67	4.02	3.66	3.66	3.68	3.66	3.66	4.11	5.45	4.56
Normal	1000	3.68	3.67	3.67	3.73	3.67	3.67	3.67	3.67	3.67	3.88	6.13	4.51
Bivariate	300	27.24	26.72	27.03	30.76	26.80	26.84	26.81	26.92	27.14	29.46	46.02	46.25
Exponential	1000	27.13	27.01	27.05	27.51	27.00	27.00	27.04	27.05	27.42	27.60	60.63	46.28
Bivariate t	300	6.97	6.83	6.86	7.62	6.82	6.83	6.83	6.82	6.82	8.62	13.13	9.04
	1000	6.83	6.80	6.80	6.92	6.80	6.79	6.80	6.79	6.79	7.86	14.64	8.98
Trivariate	300	10.24	9.27	9.37	9.34	9.26	9.38	9.35	9.27	9.28	10.23	22.90	13.15
Normal($\Sigma = \mathbf{I}_3$)	1000	9.77	9.45	9.47	9.46	9.45	9.47	9.50	9.44	9.45	10.06	30.50	12.95
Trivariate	300	8.54	7.75	7.79	7.79	7.75	7.81	7.83	7.75	7.74	10.24	23.35	15.40
Normal ($\Sigma \neq \mathbf{I}_3$)	1000	8.16	7.96	7.97	7.97	7.96	7.97	7.99	7.95	7.95	10.05	31.14	15.09
Trivariate t	300	28.09	21.67	22.07	21.70	21.65	22.20	21.80	21.76	21.74	27.39	133.59	28.58
	1000	24.39	22.54	22.65	22.58	22.55	22.63	22.61	22.55	22.53	26.34	233.60	27.85
Trivariate	300	2.76^{05}	3.48^{03}	3.27^{03}	3.39^{03}	3.46^{03}	3.60^{03}	3.16^{03}	3.38^{03}	3.32^{03}	1.70^{04}	4.14^{11}	7.51^{12}
Cauchy	1000	2.16^{04}	3.40^{03}	2.91^{03}	3.11^{03}	3.35^{03}	3.31^{03}	2.84^{03}	3.16^{03}	2.93^{03}	1.00^{04}	4.85^{10}	4.96^{10}

Table 6. Coverage probabilities of $(0.95, 0.90)$ hyperrectangular tolerance regions (top-half of table) and 0.95-expectation hyperrectangular tolerance regions (bottom-half of table).

$(0.95, 0.90)$ **Hyperrectangular Tolerance Regions**													
Distribution	n	**Simp**	**Mah**	**Tukey**	**Oja**	**Spat**	**Zon**	**Proj**	**Ellip**	**Spher**	**Bonf**	**CHull**	**Norm**
Bivariate	300	0.922	0.918	0.919	0.931	0.918	0.922	0.920	0.918	0.925	1.000	0.907	0.022
Normal	1000	0.927	0.906	0.920	0.917	0.912	0.903	0.915	0.904	0.914	1.000	1.000	0.000
Bivariate	300	0.934	0.942	0.934	0.941	0.938	0.932	0.943	0.938	0.941	1.000	0.916	0.987
Exponential	1000	0.917	0.919	0.905	0.929	0.918	0.903	0.926	0.926	0.926	0.999	0.999	1.000
Bivariate t	300	0.938	0.933	0.935	0.927	0.927	0.930	0.937	0.927	0.931	0.999	0.856	0.048
	1000	0.930	0.920	0.921	0.931	0.917	0.911	0.923	0.925	0.918	1.000	0.999	0.022
Trivariate	300	0.957	0.948	0.952	0.946	0.947	0.957	0.955	0.941	0.945	0.999	0.997	0.232
Normal($\Sigma = \mathbf{I}_3$)	1000	0.924	0.908	0.907	0.902	0.904	0.909	0.917	0.902	0.907	1.000	1.000	0.300
Trivariate	300	0.953	0.930	0.931	0.939	0.925	0.957	0.938	0.926	0.925	0.998	0.996	0.686
Normal ($\Sigma \neq \mathbf{I}_3$)	1000	0.943	0.903	0.907	0.905	0.902	0.895	0.914	0.900	0.909	1.000	1.000	0.947
Trivariate t	300	0.952	0.940	0.937	0.930	0.933	0.950	0.938	0.939	0.939	1.000	1.000	0.037
	1000	0.940	0.924	0.919	0.923	0.925	0.920	0.916	0.921	0.927	1.000	1.000	0.051
Trivariate	300	0.980	0.960	0.962	0.961	0.959	0.964	0.965	0.963	0.961	0.999	0.997	0.862
Cauchy	1000	0.952	0.927	0.913	0.920	0.925	0.909	0.919	0.910	0.920	1.000	1.000	0.992

0.90-Expectation Hyperrectangular Tolerance Regions													
Distribution	n	**Simp**	**Mah**	**Tukey**	**Oja**	**Spat**	**Zon**	**Proj**	**Ellip**	**Spher**	**Bonf**	**CHull**	**Norm**
Bivariate	300	0.891	0.889	0.890	0.890	0.889	0.888	0.890	0.889	0.889	0.910	0.930	0.885
Normal	1000	0.897	0.897	0.897	0.897	0.897	0.897	0.897	0.897	0.897	0.909	0.937	0.886
Bivariate	300	0.890	0.890	0.889	0.890	0.890	0.888	0.890	0.890	0.889	0.903	0.919	0.946
Exponential	1000	0.897	0.897	0.897	0.897	0.897	0.896	0.897	0.897	0.897	0.903	0.928	0.949
Bivariate t	300	0.891	0.889	0.890	0.890	0.889	0.889	0.890	0.889	0.889	0.916	0.917	0.895
	1000	0.897	0.897	0.897	0.897	0.897	0.896	0.897	0.896	0.896	0.917	0.925	0.900
Trivariate	300	0.884	0.882	0.883	0.882	0.881	0.882	0.883	0.881	0.882	0.904	0.973	0.876
Normal($\Sigma = \mathbf{I}_3$)	1000	0.895	0.894	0.894	0.894	0.894	0.894	0.895	0.894	0.894	0.905	0.985	0.877
Trivariate	300	0.886	0.882	0.883	0.882	0.882	0.883	0.883	0.882	0.881	0.924	0.977	0.932
Normal ($\Sigma \neq \mathbf{I}_3$)	1000	0.895	0.894	0.894	0.894	0.894	0.894	0.895	0.894	0.894	0.924	0.988	0.933
Trivariate t	300	0.886	0.883	0.883	0.883	0.882	0.882	0.883	0.882	0.882	0.915	0.974	0.879
	1000	0.895	0.895	0.895	0.895	0.895	0.894	0.895	0.895	0.895	0.916	0.983	0.881
Trivariate	300	0.888	0.885	0.884	0.885	0.885	0.885	0.884	0.884	0.884	0.941	0.977	0.969
Cauchy	1000	0.896	0.896	0.895	0.896	0.895	0.895	0.895	0.895	0.895	0.944	0.969	0.983

Table 7. Expected volumes of $(0.95, 0.90)$ hyperrectangular tolerance regions (top-half of table) and 0.95-expectation hyperrectangular tolerance regions (bottom-half of table). Here, we use $a^b \equiv a \times 10^b$ as short-hand for scientific notation.

$(0.95, 0.90)$ **Hyperrectangular Tolerance Regions**													
Distribution	n	**Simp**	**Mah**	**Tukey**	**Oja**	**Spat**	**Zon**	**Proj**	**Ellip**	**Spher**	**Bonf**	**CHull**	**Norm**
Bivariate	300	23.72	23.29	23.63	25.53	23.26	23.87	23.46	23.35	23.36	33.39	23.87	16.73
Normal	1000	21.43	21.12	21.21	21.86	21.11	21.15	21.19	21.11	21.12	23.60	26.36	17.29
Bivariate	300	48.12	38.48	47.75	42.89	38.73	49.49	38.83	39.71	40.03	78.77	53.57	40.99
Exponential	1000	54.68	31.15	43.03	31.85	31.18	44.97	31.28	31.35	31.86	47.67	63.35	43.48
Bivariate t	300	66.62	62.41	65.05	70.01	62.61	66.48	62.67	64.67	64.57	170.59	61.10	33.22
	1000	52.55	50.71	51.26	51.85	50.77	51.22	50.73	50.93	50.85	67.52	67.52	34.40
Trivariate	300	156.23	142.11	143.75	142.85	141.87	152.79	143.54	141.93	142.09	191.65	183.57	93.61
Normal($\Sigma = \mathbf{I}_3$)	1000	137.09	121.26	121.91	121.61	121.07	122.01	122.09	120.99	121.04	141.70	247.45	97.92
Trivariate	300	148.98	133.27	134.38	134.17	132.95	144.52	134.27	133.34	133.33	192.55	185.61	109.84
Normal ($\Sigma \neq \mathbf{I}_3$)	1000	124.70	109.80	110.63	110.07	109.70	110.61	110.28	109.73	110.01	141.97	253.82	113.71
Trivariate t	300	750.91	537.22	541.10	538.99	535.65	616.84	542.15	558.75	564.91	1.24^{03}	1.13^{03}	202.35
	1000	531.94	388.96	395.65	389.05	388.99	398.17	390.20	391.87	391.45	582.20	2.10^{03}	208.93
Trivariate	300	7.86^{10}	2.59^{06}	2.28^{06}	2.02^{09}	3.39^{06}	2.60^{09}	1.99^{06}	3.54^{06}	5.69^{06}	1.47^{13}	1.25^{13}	3.84^{11}
Cauchy	1000	6.52^{10}	2.31^{05}	1.94^{05}	2.41^{05}	2.28^{05}	2.63^{05}	1.75^{05}	2.20^{05}	2.02^{05}	5.11^{06}	1.32^{12}	5.37^{13}

0.90-Expectation Hyperrectangular Tolerance Regions													
Distribution	n	**Simp**	**Mah**	**Tukey**	**Oja**	**Spat**	**Zon**	**Proj**	**Ellip**	**Spher**	**Bonf**	**CHull**	**Norm**
Bivariate	300	14.49	14.19	14.32	17.07	14.20	14.24	14.31	14.22	14.22	15.81	18.12	13.98
Normal	1000	14.64	14.55	14.59	15.02	14.55	14.56	14.58	14.55	14.54	15.50	18.24	13.88
Bivariate	300	31.74	17.49	26.29	21.23	17.65	27.74	17.51	17.82	18.81	26.95	38.49	32.07
Exponential	1000	33.19	17.63	26.84	17.95	17.69	28.55	17.65	17.74	18.77	26.67	41.19	32.17
Bivariate t	300	26.87	25.83	26.20	32.52	25.87	26.19	25.86	25.96	25.98	32.80	33.88	27.75
	1000	26.87	26.62	26.70	27.46	26.62	26.66	26.62	26.62	26.59	31.44	34.24	27.61
Trivariate	300	81.91	70.67	71.64	71.30	70.59	71.77	71.47	70.62	70.70	82.05	170.64	74.92
Normal($\Sigma = \mathbf{I}_3$)	1000	77.75	74.06	74.28	74.21	74.02	74.25	74.43	74.00	74.03	78.83	209.15	74.09
Trivariate	300	71.71	59.97	60.74	60.54	59.97	60.82	60.48	59.92	59.76	82.12	173.93	87.90
Normal ($\Sigma \neq \mathbf{I}_3$)	1000	65.55	63.05	63.34	63.16	63.07	63.20	63.36	63.06	63.02	78.73	218.73	86.34
Trivariate t	300	226.94	155.32	157.94	155.64	155.40	159.39	156.16	156.14	155.48	227.46	948.65	162.33
	1000	184.37	165.41	166.51	165.57	165.36	166.42	165.90	165.32	165.35	206.77	1.19^{03}	159.77
Trivariate	300	4.37^{11}	1.03^{04}	8.76^{03}	1.01^{04}	9.94^{03}	1.16^{04}	7.73^{03}	9.77^{03}	9.12^{03}	1.74^{05}	1.42^{12}	4.41^{10}
Cauchy	1000	2.07^{04}	1.21^{04}	9.24^{03}	1.08^{04}	1.16^{04}	1.24^{04}	8.89^{03}	1.07^{04}	9.23^{03}	7.38^{04}	3.84^{11}	3.91^{12}

Table 8. Coverage probabilities of $(0.95, 0.90)$ upper semi-space tolerance regions (top-half of table) and 0.90-expectation upper semi-space tolerance regions (bottom-half of table).

$(0.95, 0.90)$ **Upper Semi-Space Tolerance Regions**													
Distribution	n	**Simp**	**Mah**	**Tukey**	**Oja**	**Spat**	**Zon**	**Proj**	**Ellip**	**Spher**	**Bonf**	**CHull**	**Norm**
Bivariate	300	0.910	0.898	0.906	0.906	0.903	0.897	0.899	0.904	0.902	0.996	0.998	0.890
Normal	1000	0.904	0.897	0.896	0.894	0.895	0.893	0.900	0.895	0.890	0.999	1.000	0.995
Bivariate	300	0.884	0.875	0.880	0.882	0.871	0.874	0.883	0.871	0.883	0.998	1.000	1.000
Exponential	1000	0.904	0.899	0.911	0.906	0.901	0.901	0.900	0.907	0.899	0.996	1.000	1.000
Bivariate t	300	0.873	0.868	0.871	0.884	0.868	0.866	0.879	0.869	0.868	0.997	0.996	0.802
	1000	0.890	0.888	0.884	0.894	0.880	0.881	0.889	0.881	0.885	1.000	1.000	0.984
Trivariate	300	0.917	0.898	0.898	0.896	0.895	0.900	0.899	0.890	0.892	1.000	1.000	0.605
Normal($\Sigma = \mathbf{I}_3$)	1000	0.917	0.911	0.909	0.908	0.910	0.908	0.913	0.906	0.914	0.999	1.000	0.671
Trivariate	300	0.907	0.891	0.894	0.889	0.889	0.897	0.895	0.894	0.899	1.000	1.000	1.000
Normal ($\Sigma \neq \mathbf{I}_3$)	1000	0.884	0.879	0.877	0.882	0.872	0.880	0.891	0.880	0.878	1.000	1.000	1.000
Trivariate t	300	0.890	0.876	0.873	0.875	0.869	0.876	0.874	0.868	0.865	1.000	1.000	0.502
	1000	0.899	0.909	0.892	0.900	0.902	0.894	0.911	0.891	0.898	1.000	1.000	0.541
Trivariate	300	0.893	0.887	0.882	0.885	0.884	0.892	0.886	0.883	0.879	1.000	1.000	0.980
Cauchy	1000	0.881	0.896	0.880	0.889	0.892	0.884	0.882	0.881	0.879	1.000	1.000	1.000

0.90-Expectation Upper Semi-Space Tolerance Regions													
Distribution	n	**Simp**	**Mah**	**Tukey**	**Oja**	**Spat**	**Zon**	**Proj**	**Ellip**	**Spher**	**Bonf**	**CHull**	**Norm**
Bivariate	300	0.897	0.897	0.897	0.897	0.897	0.897	0.897	0.897	0.897	0.913	0.966	0.943
Normal	1000	0.899	0.899	0.899	0.899	0.899	0.899	0.899	0.899	0.899	0.912	0.969	0.943
Bivariate	300	0.897	0.896	0.897	0.896	0.896	0.896	0.896	0.896	0.897	0.903	0.971	0.963
Exponential	1000	0.899	0.899	0.899	0.899	0.899	0.899	0.899	0.899	0.900	0.903	0.978	0.964
Bivariate t	300	0.897	0.897	0.897	0.897	0.897	0.896	0.897	0.897	0.897	0.917	0.958	0.947
	1000	0.898	0.898	0.898	0.899	0.898	0.898	0.898	0.898	0.898	0.917	0.962	0.949
Trivariate	300	0.895	0.893	0.894	0.893	0.893	0.894	0.894	0.893	0.894	0.905	0.986	0.937
Normal($\Sigma = \mathbf{I}_3$)	1000	0.899	0.898	0.898	0.898	0.898	0.898	0.898	0.898	0.898	0.905	0.992	0.937
Trivariate	300	0.895	0.894	0.894	0.894	0.894	0.894	0.894	0.894	0.894	0.928	0.989	0.966
Normal ($\Sigma \neq \mathbf{I}_3$)	1000	0.898	0.898	0.898	0.898	0.898	0.898	0.898	0.898	0.898	0.929	0.994	0.966
Trivariate t	300	0.894	0.892	0.893	0.893	0.892	0.892	0.893	0.892	0.892	0.909	0.987	0.934
	1000	0.898	0.898	0.898	0.898	0.898	0.898	0.898	0.898	0.898	0.910	0.991	0.935
Trivariate	300	0.894	0.894	0.894	0.894	0.894	0.893	0.894	0.894	0.894	0.925	0.985	0.980
Cauchy	1000	0.898	0.898	0.898	0.898	0.898	0.898	0.898	0.898	0.898	0.926	0.980	0.989

Table 9. Expected volumes of $(0.95, 0.90)$ upper semi-space tolerance regions (top-half of table) and 0.95-expectation upper semi-space tolerance regions (bottom-half of table). Here, we use $a^b \equiv a \times 10^b$ as short-hand for scientific notation.

$(0.95, 0.90)$ **Upper Semi-Space Tolerance Regions**													
Distribution	n	**Simp**	**Mah**	**Tukey**	**Oja**	**Spat**	**Zon**	**Proj**	**Ellip**	**Spher**	**Bonf**	**CHull**	**Norm**
Bivariate	300	4.43	4.36	4.38	4.73	4.35	4.37	4.38	4.36	4.36	5.73	6.00	4.19
Normal	1000	4.03	4.01	4.01	4.08	4.01	4.01	4.02	4.01	4.01	4.55	6.63	4.32
Bivariate	300	33.86	32.88	33.44	37.12	32.98	33.16	33.02	33.28	33.46	46.00	53.75	41.04
Exponential	1000	30.21	29.98	30.07	30.64	29.98	30.00	30.09	30.05	30.42	33.80	63.58	43.51
Bivariate t	300	9.35	9.07	9.13	9.97	9.07	9.10	9.07	9.09	9.04	16.30	15.41	8.30
	1000	7.93	7.88	7.88	7.99	7.87	7.87	7.88	7.86	7.86	10.29	16.97	8.60
Trivariate	300	13.11	11.99	12.11	12.06	11.96	12.23	12.10	11.97	11.96	24.27	23.25	11.71
Normal($\Sigma = \mathbf{I}_3$)	1000	11.35	10.80	10.86	10.83	10.80	10.84	10.87	10.80	10.81	12.89	31.16	12.23
Trivariate	300	11.53	10.56	10.62	10.60	10.57	10.72	10.66	10.57	10.52	24.58	23.80	13.69
Normal ($\Sigma \neq \mathbf{I}_3$)	1000	9.52	9.19	9.21	9.20	9.18	9.20	9.23	9.18	9.19	12.96	32.11	14.26
Trivariate t	300	43.14	33.69	34.22	33.79	33.60	35.12	33.88	33.95	33.96	157.92	143.02	25.55
	1000	31.29	27.65	27.73	27.68	27.65	27.77	27.71	27.63	27.59	40.12	267.44	26.22
Trivariate	300	7.58^{05}	1.74^{04}	1.66^{04}	1.69^{04}	1.72^{04}	1.84^{04}	1.56^{04}	1.76^{04}	1.70^{04}	1.01^{10}	1.00^{10}	7.02^{11}
Cauchy	1000	1.93^{04}	6.72^{03}	5.75^{03}	6.16^{03}	6.52^{03}	6.49^{03}	5.71^{03}	6.21^{03}	5.78^{03}	4.88^{04}	1.06^{10}	5.34^{13}

0.90-Expectation Upper Semi-Space Tolerance Regions													
Distribution	n	**Simp**	**Mah**	**Tukey**	**Oja**	**Spat**	**Zon**	**Proj**	**Ellip**	**Spher**	**Bonf**	**CHull**	**Norm**
Bivariate	300	2.49	2.47	2.48	2.74	2.47	2.47	2.47	2.47	2.47	2.76	4.56	3.50
Normal	1000	2.49	2.49	2.49	2.53	2.49	2.49	2.49	2.49	2.49	2.72	4.57	3.47
Bivariate	300	17.69	17.53	17.60	20.40	17.55	17.54	17.54	17.57	17.74	18.40	38.97	32.21
Exponential	1000	17.69	17.64	17.66	17.95	17.64	17.64	17.66	17.65	17.98	18.13	41.66	32.30
Bivariate t	300	3.88	3.85	3.85	4.38	3.85	3.84	3.84	3.84	3.83	4.72	8.53	6.93
	1000	3.83	3.83	3.83	3.90	3.82	3.82	3.83	3.82	3.82	4.58	8.56	6.90
Trivariate	300	6.50	5.87	5.90	5.90	5.87	5.89	5.90	5.87	5.87	6.42	21.31	9.37
Normal($\Sigma = \mathbf{I}_3$)	1000	6.05	5.98	5.99	5.99	5.98	5.99	6.00	5.98	5.98	6.30	26.14	9.25
Trivariate	300	4.94	4.52	4.54	4.54	4.53	4.54	4.55	4.53	4.51	6.42	22.21	11.04
Normal ($\Sigma \neq \mathbf{I}_3$)	1000	4.63	4.59	4.60	4.60	4.59	4.59	4.61	4.59	4.59	6.30	27.83	10.79
Trivariate t	300	13.27	11.09	11.14	11.14	11.08	11.15	11.13	11.09	11.06	13.51	122.84	20.23
	1000	11.47	11.37	11.37	11.36	11.35	11.37	11.37	11.35	11.34	13.09	146.58	19.79
Trivariate	300	7.61^{03}	418.35	373.83	400.13	408.20	410.37	360.36	398.66	373.51	1.33^{03}	1.00^{10}	2.71^{11}
Cauchy	1000	361.44	440.35	354.17	391.70	420.41	412.49	352.13	399.64	352.14	996.02	2.45^{10}	1.01^{13}

10 Additional Results for the Kidney Function Example

The published reference limit for UACR is an upper bound of 30.0 mg/g for both adult males and females. Using our nonparametric tolerance regions procedure, the calculated reference regions for adolescent males and females are both noticeably lower. This suggests that not only should a different reference limit be used based on the subject's gender, but that perhaps the larger published reference limit for adults is too conservative for flagging a subject's risk of kidney disease when the subject is an adolescent.

SC is a reliable indicator of kidney function, with abnormally high levels being an especially strong indicator of possible kidney failure. The published reference intervals for adult males and females are relatively similar. The reference intervals determined using our nonparametric tolerance regions approach are also similar to each other, and both intervals are only slightly more conservative than the published intervals.

We also calculated nonparametric $(0.95, 0.95)$ and 0.95-expectation semi-space tolerance regions based on five of the other eight depth functions discussed in this paper. The regions based on the simplicial, Oja, and projection depth were not calculated since the large reference sample sizes necessitate the use of approximation algorithms for these depth calculations. To achieve a practical order of computation with these depth functions, we would have to use a relatively small proportion (e.g., 1%) of the computed depth geometries based on the approximations used in the `ddalpha` package. These could yield misleading limits in our routine and, thus, are not investigated for this application. Regardless, the additional results for the other five depth functions appear below. We found that the limits for the tolerance regions pertaining to UA and SC are fairly consistent, regardless of the depth function used. However, there is some variability in the upper tolerance limit calculated for UACR, which is due to the heavy right-skewness of this particular analyte. These relatively small differences are consistent with what we noted in the main text about the impact of different depth functions on nonparametric tests and nonparametric descriptions of data.

Table 10. Summary of reference regions for the analytes UACR, UA, and SC. Given are the published reference intervals for adult males (top-half) and adult females (bottom-half), the calculated nonparametric $(0.95, 0.95)$ and 0.95-expectation semi-space tolerance regions for adolescent males (top-half) and adolescent females (bottom-half) using the reference sample. The nonparametric regions were calculated using Mahalanobis depth.

Analyte	Published Reference Interval (Adult)	$(0.95, 0.95)$ Tolerance Region (Adolescent)	0.95-Expectation Tolerance Region (Adolescent)
Males			
UACR	≤ 30.0 mg/g	≤ 3.1 mg/g	≤ 3.1 mg/g
UA	$3.4 - 7.2$ mg/dL	$2.6 - 8.1$ mg/dL	$2.7 - 7.9$ mg/dL
SC	$0.7 - 1.2$ mg/dL	$0.3 - 1.2$ mg/dL	$0.3 - 1.2$ mg/dL
Females			
UACR	≤ 30.0 mg/g	≤ 3.3 mg/g	≤ 3.0 mg/g
UA	$2.4 - 6.1$ mg/dL	$2.2 - 6.5$ mg/dL	$2.3 - 6.3$ mg/dL
SC	$0.5 - 1.0$ mg/dL	$0.3 - 1.0$ mg/dL	$0.3 - 1.0$ mg/dL

Table 11. Summary of reference regions for the analytes UACR, UA, and SC. Given are the published reference intervals for adult males (top-half) and adult females (bottom-half), the calculated nonparametric $(0.95, 0.95)$ and 0.95-expectation semi-space tolerance regions for adolescent males (top-half) and adolescent females (bottom-half) using the reference sample. The nonparametric regions were calculated using Tukey depth.

Analyte	Published Reference Interval (Adult)	$(0.95, 0.95)$ Tolerance Region (Adolescent)	0.95-Expectation Tolerance Region (Adolescent)
		Males	
UACR	≤ 30.0 mg/g	≤ 4.6 mg/g	≤ 3.5 mg/g
UA	$3.4 - 7.2$ mg/dL	$2.9 - 8.1$ mg/dL	$2.9 - 8.1$ mg/dL
SC	$0.7 - 1.2$ mg/dL	$0.3 - 1.2$ mg/dL	$0.4 - 1.2$ mg/dL
		Females	
UACR	≤ 30.0 mg/g	≤ 5.2 mg/g	≤ 4.3 mg/g
UA	$2.4 - 6.1$ mg/dL	$2.5 - 6.8$ mg/dL	$2.5 - 6.5$ mg/dL
SC	$0.5 - 1.0$ mg/dL	$0.3 - 1.0$ mg/dL	$0.3 - 1.0$ mg/dL

Table 12. Summary of reference regions for the analytes UACR, UA, and SC. Given are the published reference intervals for adult males (top-half) and adult females (bottom-half), the calculated nonparametric $(0.95, 0.95)$ and 0.95-expectation semi-space tolerance regions for adolescent males (top-half) and adolescent females (bottom-half) using the reference sample. The nonparametric regions were calculated using spatial depth.

Analyte	Published Reference Interval (Adult)	$(0.95, 0.95)$ Tolerance Region (Adolescent)	0.95-Expectation Tolerance Region (Adolescent)
		Males	
UACR	≤ 30.0 mg/g	≤ 3.5 mg/g	≤ 3.5 mg/g
UA	$3.4 - 7.2$ mg/dL	$2.8 - 8.1$ mg/dL	$2.8 - 8.0$ mg/dL
SC	$0.7 - 1.2$ mg/dL	$0.3 - 1.2$ mg/dL	$0.3 - 1.2$ mg/dL
		Females	
UACR	≤ 30.0 mg/g	≤ 3.7 mg/g	≤ 3.6 mg/g
UA	$2.4 - 6.1$ mg/dL	$2.3 - 6.5$ mg/dL	$2.4 - 6.3$ mg/dL
SC	$0.5 - 1.0$ mg/dL	$0.3 - 1.0$ mg/dL	$0.3 - 1.0$ mg/dL

Table 13. Summary of reference regions for the analytes UACR, UA, and SC. Given are the published reference intervals for adult males (top-half) and adult females (bottom-half), the calculated nonparametric $(0.95, 0.95)$ and 0.95-expectation semi-space tolerance regions for adolescent males (top-half) and adolescent females (bottom-half) using the reference sample. The nonparametric regions were calculated using zonoid depth.

Analyte	Published Reference Interval (Adult)	$(0.95, 0.95)$ Tolerance Region (Adolescent)	0.95-Expectation Tolerance Region (Adolescent)
Males			
UACR	≤ 30.0 mg/g	≤ 6.4 mg/g	≤ 4.6 mg/g
UA	$3.4 - 7.2$ mg/dL	$2.9.8.4$ mg/dL	$3.0 - 8.1$ mg/dL
SC	$0.7 - 1.2$ mg/dL	$0.4 - 1.2$ mg/dL	$0.4 - 1.2$ mg/dL
Females			
UACR	≤ 30.0 mg/g	≤ 5.9 mg/g	≤ 5.9 mg/g
UA	$2.4 - 6.1$ mg/dL	$2.4 - 6.8$ mg/dL	$2.5 - 6.6$ mg/dL
SC	$0.5 - 1.0$ mg/dL	$0.4 - 1.0$ mg/dL	$0.4 - 1.0$ mg/dL

Table 14. Summary of reference regions for the analytes UACR, UA, and SC. Given are the published reference intervals for adult males (top-half) and adult females (bottom-half), the calculated nonparametric $(0.95, 0.95)$ and 0.95-expectation semi-space tolerance regions for adolescent males (top-half) and adolescent females (bottom-half) using the reference sample. The nonparametric regions were calculated using spherical depth.

Analyte	Published Reference Interval (Adult)	$(0.95, 0.95)$ Tolerance Region (Adolescent)	0.95-Expectation Tolerance Region (Adolescent)
Males			
UACR	≤ 30.0 mg/g	≤ 3.1 mg/g	≤ 2.5 mg/g
UA	$3.4 - 7.2$ mg/dL	$3.0 - 7.9$ mg/dL	$3.1 - 7.8$ mg/dL
SC	$0.7 - 1.2$ mg/dL	$0.2 - 1.5$ mg/dL	$0.2 - 1.5$ mg/dL
Females			
UACR	≤ 30.0 mg/g	≤ 3.9 mg/g	≤ 3.3 mg/g
UA	$2.4 - 6.1$ mg/dL	$2.5 - 6.5$ mg/dL	$2.6 - 6.3$ mg/dL
SC	$0.5 - 1.0$ mg/dL	$0.2 - 1.1$ mg/dL	$0.2 - 1.1$ mg/dL

Table 15. Summary of reference regions for the analytes UACR, UA, and SC. Given are the published reference intervals for adult males (top-half) and adult females (bottom-half), the calculated nonparametric $(0.95, 0.95)$ and 0.95-expectation semi-space tolerance regions for adolescent males (top-half) and adolescent females (bottom-half) using the reference sample. The nonparametric regions were calculated using the Bonferroni correction method.

Analyte	Published Reference Interval (Adult)	$(0.95, 0.95)$ Tolerance Region (Adolescent)	0.95-Expectation Tolerance Region (Adolescent)
		Males	
UACR	≤ 30.0 mg/g	≤ 3.4 mg/g	≤ 2.4 mg/g
UA	$3.4 - 7.2$ mg/dL	$2.6 - 8.5$ mg/dL	$2.8 - 8.2$ mg/dL
SC	$0.7 - 1.2$ mg/dL	$0.2 - 1.2$ mg/dL	$0.3 - 1.2$ mg/dL
		Females	
UACR	≤ 30.0 mg/g	≤ 4.7 mg/g	≤ 3.7 mg/g
UA	$2.4 - 6.1$ mg/dL	$2.3 - 6.9$ mg/dL	$2.4 - 6.7$ mg/dL
SC	$0.5 - 1.0$ mg/dL	$0.3 - 1.0$ mg/dL	$0.3 - 1.0$ mg/dL

Table 16. Summary of reference regions for the analytes UACR, UA, and SC. Given are the published reference intervals for adult males (top-half) and adult females (bottom-half), the calculated nonparametric $(0.95, 0.95)$ and 0.95-expectation semi-space tolerance regions for adolescent males (top-half) and adolescent females (bottom-half) using the reference sample. The nonparametric regions were calculated using a bounding region based on the convex hull approach.

Analyte	Published Reference Interval (Adult)	$(0.95, 0.95)$ Tolerance Region (Adolescent)	0.95-Expectation Tolerance Region (Adolescent)
		Males	
UACR	≤ 30.0 mg/g	≤ 36.9 mg/g	≤ 36.9 mg/g
UA	$3.4 - 7.2$ mg/dL	$2.2 - 14.9$ mg/dL	$2.3 - 9.5$ mg/dL
SC	$0.7 - 1.2$ mg/dL	$0.3 - 1.3$ mg/dL	$0.2 - 1.3$ mg/dL
		Females	
UACR	≤ 30.0 mg/g	≤ 30.0 mg/g	≤ 17.1 mg/g
UA	$2.4 - 6.1$ mg/dL	$1.8 - 8.5$ mg/dL	$1.8 - 8.1$ mg/dL
SC	$0.5 - 1.0$ mg/dL	$0.2 - 5.0$ mg/dL	$0.2 - 5.0$ mg/dL

Table 17. Summary of reference regions for the analytes UACR, UA, and SC. Given are the published reference intervals for adult males (top-half) and adult females (bottom-half), the calculated nonparametric $(0.95, 0.95)$ and 0.95-expectation semi-space tolerance regions for adolescent males (top-half) and adolescent females (bottom-half) using the reference sample. The nonparametric regions were calculated using a bounding region based on the multivariate normal tolerance region.

Analyte	Published Reference Interval (Adult)	$(0.95, 0.95)$ Tolerance Region (Adolescent)	0.95-Expectation Tolerance Region (Adolescent)
Males			
UACR	≤ 30.0 mg/g	≤ 1.6 mg/g	≤ 1.7 mg/g
UA	$3.4 - 7.2$ mg/dL	$2.7 - 9.0$ mg/dL	$2.7 - 9.0$ mg/dL
SC	$0.7 - 1.2$ mg/dL	$0.4 - 1.2$ mg/dL	$0.4 - 1.2$ mg/dL
Females			
UACR	≤ 30.0 mg/g	≤ 2.3 mg/g	≤ 2.3 mg/g
UA	$2.4 - 6.1$ mg/dL	$2.3 - 7.1$ mg/dL	$2.3 - 7.1$ mg/dL
SC	$0.5 - 1.0$ mg/dL	$0.3 - 1.1$ mg/dL	$0.3 - 1.1$ mg/dL

Table 18. Summary of reference regions for the analytes UACR, UA, and SC. These results are for the adult population from NHANES. The top-half of the table are the results for the adult males. The bottom-half of the table are the results for the adult females. Six of the depth-based regions are reported, as well as the Bonferroni approach, the hyperrectangular region based on the convex hull approach, and the hyperrectangular region based on the multivariate normal tolerance region.

Analyte	Published	Elliptical	Maha-lanobis	Tukey	Spatial	Zonoid	Spherical	Bonfer-roni	Convex Hull	Normal
Adult Males										
$(0.95, 0.95)$ **Tolerance Regions**										
UACR (mg/g)	≤ 30.0	≤ 0.8	≤ 1.1	≤ 0.7	≤ 1.1	≤ 1.0	≤ 1.4	≤ 0.5	≤ 3.4	≤ 0.4
UA (mg/dL)	$3.4 - 7.2$	$3.4 - 8.5$	$3.2 - 8.4$	$3.5 - 8.7$	$3.4 - 8.4$	$3.5 - 8.6$	$3.8 - 8.3$	$3.3 - 8.9$	$2.7 - 10.4$	$3.2 - 9.3$
SC (mg/dL)	$0.7 - 1.2$	$0.6 - 1.3$	$0.6 - 1.3$	$0.6 - 1.4$	$0.6 - 1.3$	$0.6 - 1.4$	$0.5 - 2.3$	$0.6 - 1.4$	$0.5 - 2.5$	$0.6 - 1.4$
0.95**-Expectation Tolerance Regions**										
UACR (mg/g)	≤ 30.0	≤ 0.8	≤ 1.1	≤ 0.5	≤ 1.1	≤ 0.9	≤ 1.4	≤ 0.4	≤ 2.2	≤ 0.4
UA (mg/dL)	$3.4 - 7.2$	$3.5 - 8.5$	$3.3 - 8.3$	$3.5 - 8.6$	$3.4 - 8.3$	$3.6 - 8.5$	$3.8 - 8.1$	$3.4 - 8.9$	$2.7 - 10.4$	$3.2 - 9.4$
SC (mg/dL)	$0.7 - 1.2$	$0.6 - 1.3$	$0.6 - 1.3$	$0.6 - 1.3$	$0.6 - 1.3$	$0.6 - 1.4$	$0.5 - 1.6$	$0.6 - 1.4$	$0.5 - 2.5$	$0.5 - 1.5$
Adult Females										
$(0.95, 0.95)$ **Tolerance Regions**										
UACR (mg/g)	≤ 30.0	≤ 1.3	≤ 1.6	≤ 1.6	≤ 1.6	≤ 2.2	≤ 1.6	≤ 1.3	≤ 28.2	≤ 0.8
UA (mg/dL)	$2.4 - 6.1$	$2.4 - 6.8$	$2.1 - 6.6$	$2.5 - 6.9$	$2.3 - 6.7$	$2.5 - 6.9$	$2.7 - 6.7$	$2.3 - 7.3$	$1.8 - 8.9$	$2.2 - 7.4$
SC (mg/dL)	$0.5 - 1.0$	$0.4 - 1.0$	$0.4 - 1.0$	$0.4 - 1.1$	$0.4 - 1.0$	$0.4 - 1.1$	$0.3 - 1.4$	$0.4 - 1.1$	$0.3 - 3.3$	$0.4 - 1.1$
0.95**-Expectation Tolerance Regions**										
UACR (mg/g)	≤ 30.0	≤ 1.3	≤ 1.5	≤ 1.3	≤ 1.6	≤ 2.1	≤ 1.6	≤ 1.1	≤ 28.2	≤ 0.9
UA (mg/dL)	$2.4 - 6.1$	$2.4 - 6.7$	$2.2 - 6.5$	$2.5 - 6.9$	$2.4 - 6.6$	$2.5 - 6.8$	$2.7 - 6.6$	$2.4 - 7.2$	$2.0 - 7.8$	$2.2 - 7.5$
SC (mg/dL)	$0.5 - 1.0$	$0.4 - 1.0$	$0.4 - 1.0$	$0.4 - 1.1$	$0.4 - 1.0$	$0.4 - 1.0$	$0.3 - 1.4$	$0.4 - 1.1$	$0.3 - 3.3$	$0.4 - 1.1$

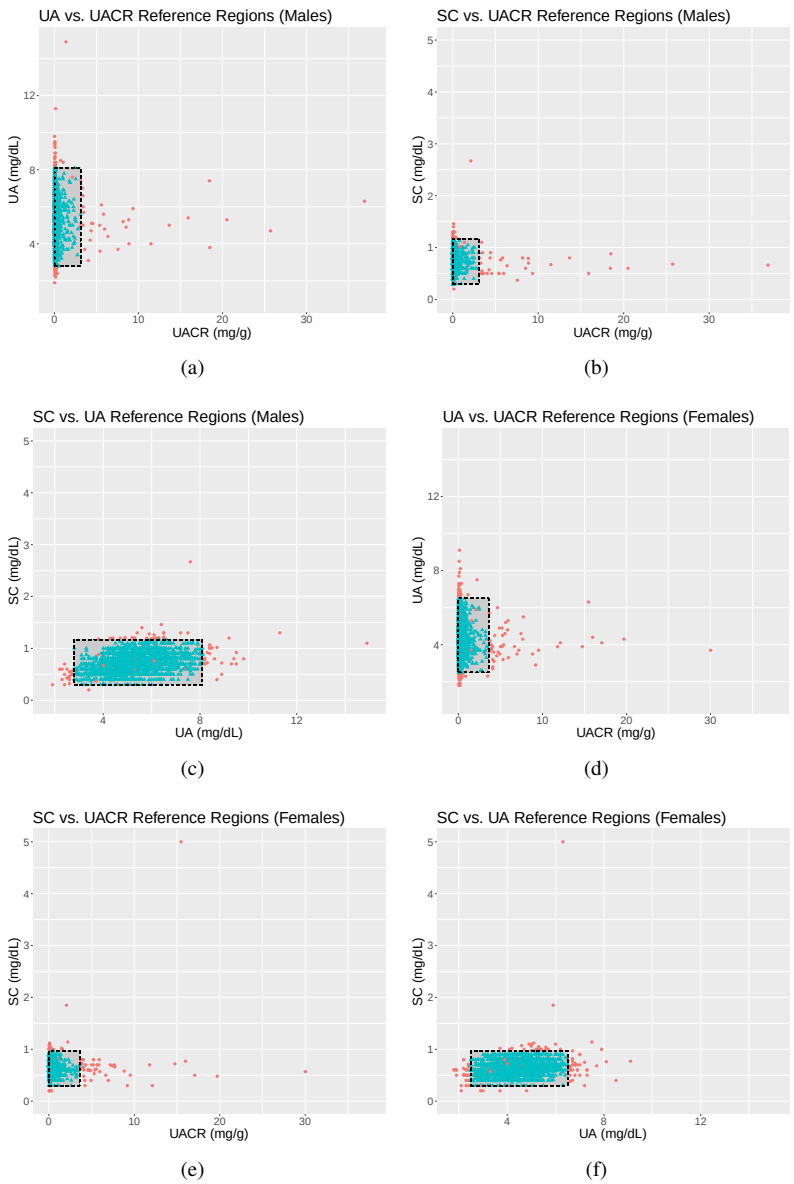

Figure 4. Pairwise scatterplots of the adolescent male reference sample ((a), (b), and (c)) and adolescent female reference sample ((d), (e), and (f)) with the nonparametric 0.95-expectation tolerance regions based on elliptical depth overlaid.

11 Additional Results for the IGF Serum Concentrations Example

In the multivariate linear regression model proposed in Mattsson et al.[30], the covariate vector $\mathbf{x}$ is taken to be the 5×1 vector $(1, \text{age} - 45, (\text{age} - 45)^2, \text{gender}, \text{BMI} - 25)^{\mathrm{T}}$, where the gender is coded as 0 for males and 1 for females. Note that the model involves an intercept. Furthermore, the trivariate response variable $\mathbf{y}$ is taken as $\mathbf{y} = (y_1, y_2, y_3)^{\mathrm{T}} = (\ln(\text{S-IGF-I}), (\text{S-IGFBP-2})^{0.25}, \ln(\text{S-IGFBP-3}))^{\mathrm{T}}$. Thus, we have the multivariate linear regression model, where $\mathbf{y}_i$ and $\mathbf{x}_i$ are the response vector and the covariate vector, respectively, for subject i, $\mathbf{B}$ is 3×5 matrix of regression parameters, and the $\boldsymbol{\epsilon}_i$ are 3-dimensional iid error vectors distributed according to $\mathcal{N}_3(\mathbf{0}_3, \boldsymbol{\Sigma})$. The dataset analyzed[30] consists of data obtained on 427 healthy individuals. The estimates for $\mathbf{B}$ and $\boldsymbol{\Sigma}$ are, respectively,

$$\hat{\mathbf{B}} = \begin{pmatrix} 4.85433 & -0.01437 & 0.00019 & -0.03486 & -0.00221 \\ 4.44923 & 0.00977 & -0.00010 & -0.04277 & -0.06545 \\ 8.07157 & -0.00434 & -0.00004 & 0.08677 & 0.00325 \end{pmatrix} \quad \text{and}$$

$$\mathbf{S} = \begin{pmatrix} 0.06982 & -0.01365 & 0.03117 \\ -0.01365 & 0.20727 & -0.01687 \\ 0.03117 & -0.01687 & 0.04098 \end{pmatrix}.$$

These are the same estimates used in Mattson et al.[30]

Figure 5 shows the full trivariate reference regions obtained in the main text plotted on the transformed scales of the responses. This figure highlights the good agreement between the two methods with capturing similar ranges in the response space. However, we again emphasize that our nonparametric procedure has a number of benefits over the normal-based confidence region approach, such as it does not require any distributional assumptions and it provides easily interpretable limits for each component of the measurement vector.

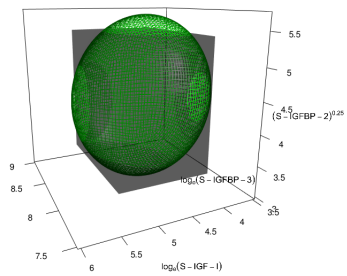

Figure 5. Full trivariate reference regions plotted on the transformed scales of the responses for males 45 years of age with a BMI of 25 kg/m^2. Both the 0.95-expectation hyperrectangular tolerance regions and 95% normal-based confidence regions are shown.

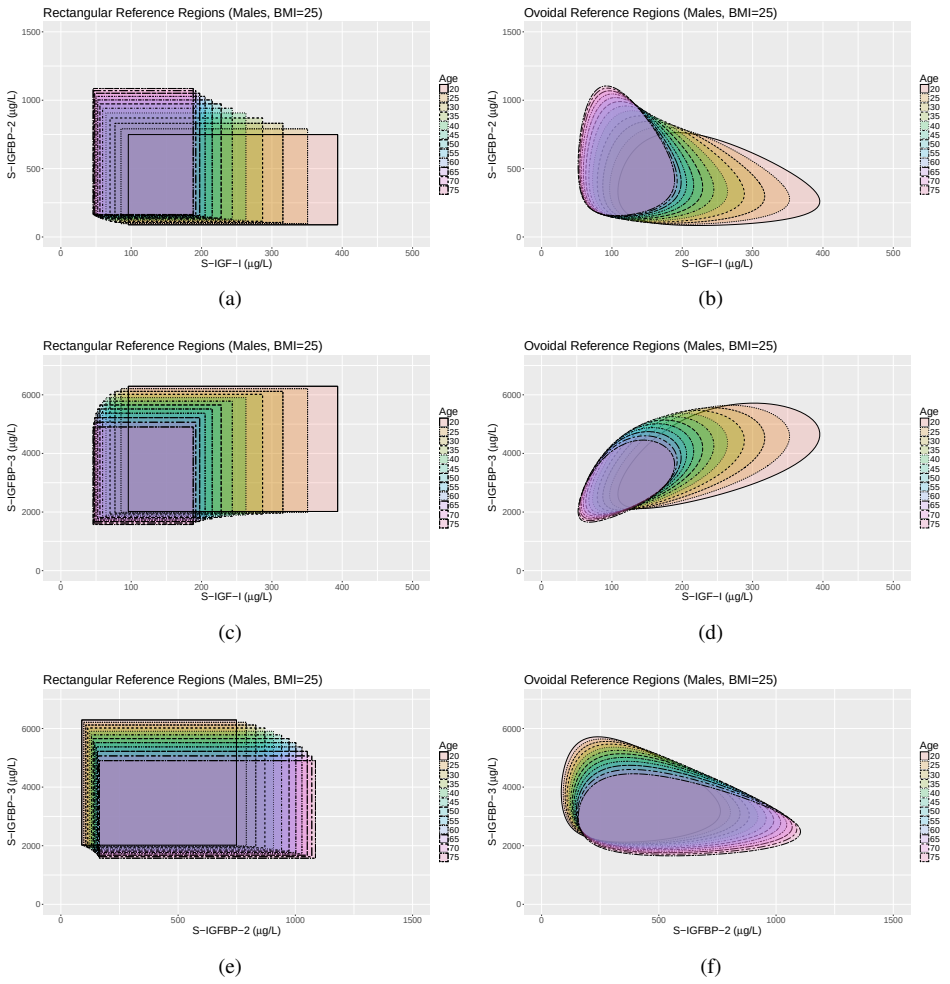

Figure 6. Pairwise plots of reference regions using $(0.95, 0.95)$ hyperrectangular tolerance regions ((a),(c), and (e)) and 95% normal-based confidence regions in Mattson et al.[30] ((b), (d), and (f)). These reference regions are for healthy males by age at a fixed BMI of 25 kg/m^2.

Finally, similar results are obtained based on the female reference sample, as well as when calculating a (P, γ) hyperrectangular tolerance region for the reference regions of interest. Below we provide similar plots as in this section for the 0.95-expectation tolerance regions based on spherical depth for healthy females by age at a fixed BMI of 25 kg/m^2 and healthy females by BMI at a fixed age of 45 years. We also report the analogous figures for the $(0.95, 0.95)$ hyperrectangular tolerance regions based on spherical depth for both healthy males and healthy females.

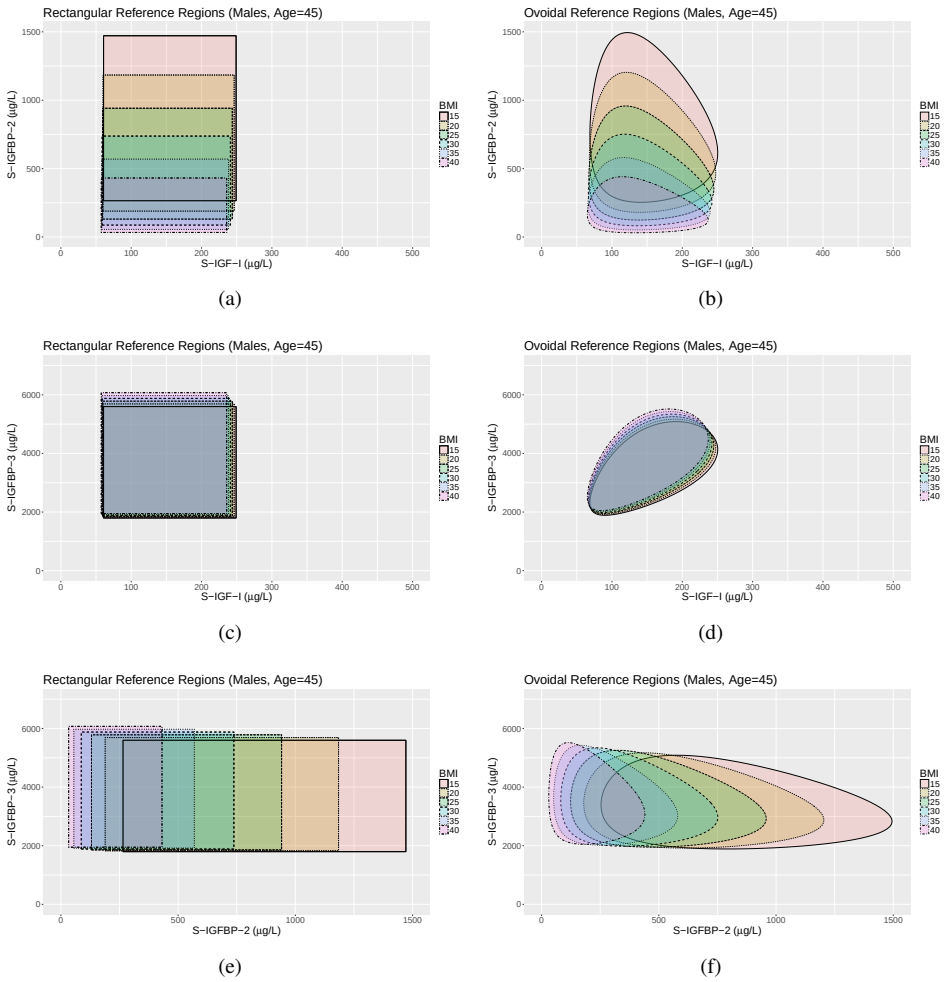

Figure 7. Pairwise plots of reference regions using $(0.95, 0.95)$ hyperrectangular tolerance regions ((a),(c), and (e)) and 95% normal-based confidence regions in Mattson et al.[30] ((b), (d), and (f)). These reference regions are for healthy males by BMI at a fixed age of 45 years.

12 Parametric Assumption

One issue of practical relevance is the construction of hyperrectangular reference regions based on a parametric assumption. Hyperrectangular tolerance regions for different multivariate distributions will each have their own computational and theoretical challenges. However, we have given some consideration to an extension of our procedure for the parametric setting. We start by constructing

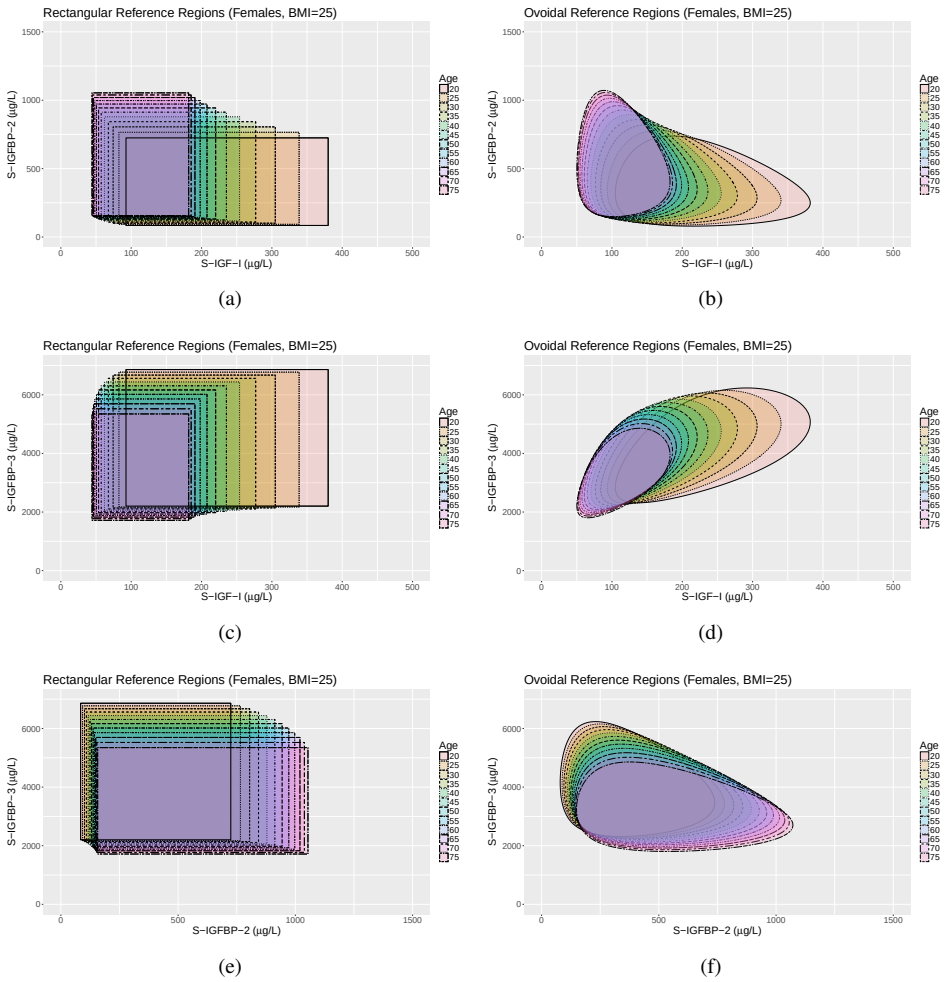

Figure 8. Pairwise plots of reference regions using $(0.95, 0.95)$ hyperrectangular tolerance regions ((a),(c), and (e)) and 95% normal-based confidence regions in ((b), (d), and (f)). These reference regions are for healthy females by age at a fixed BMI of 25 kg/m^2.

joint parametric tolerance intervals with an error correction; e.g., Bonferroni or Šidák correction. These error corrections will result in conservative coverage probabilities. We then apply a bootstrap calibration – see Chapter 18 of Efron and Tibshirani [31] – to ensure we achieve coverage probabilities as close to nominal as possible. We conducted a small simulation study where we simulated datasets

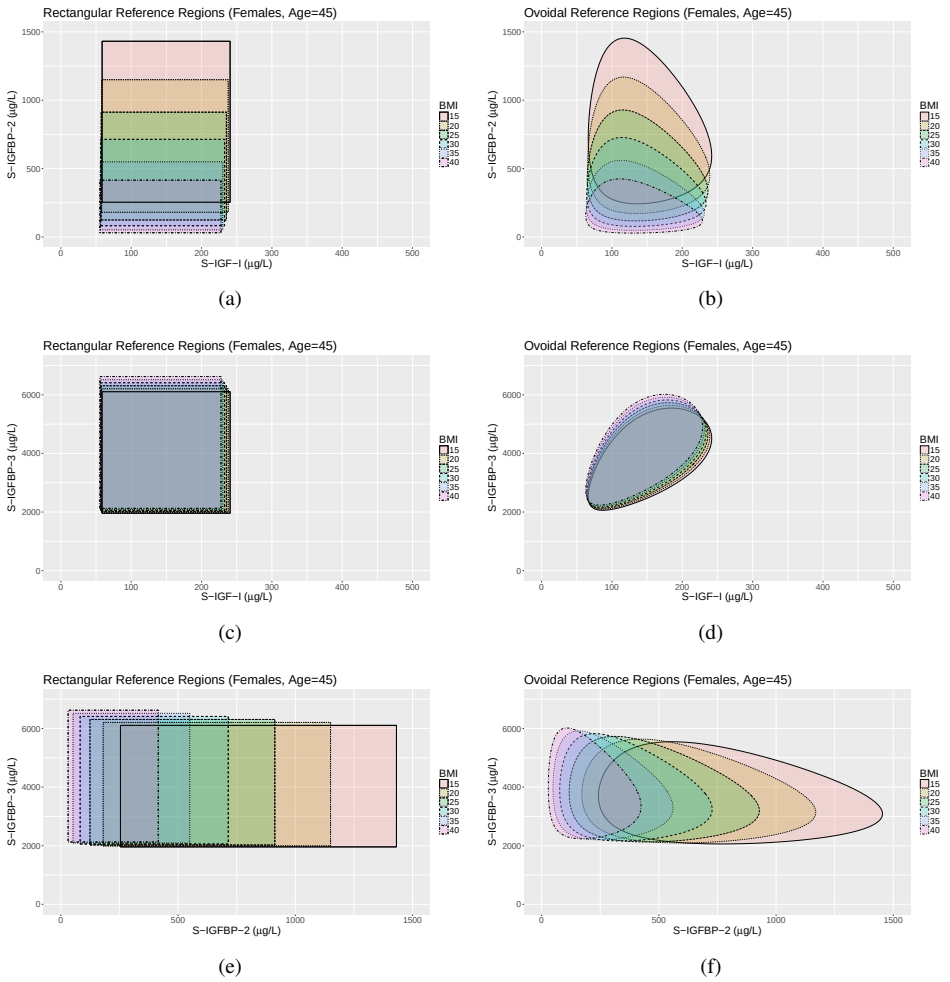

Figure 9. Pairwise plots of reference regions using $(0.95, 0.95)$ hyperrectangular tolerance regions ((a),(c), and (e)) and 95% normal-based confidence regions in ((b), (d), and (f)). These reference regions are for healthy females by BMI at a fixed age of 45 years.

of size $n \in \{50, 150\}$ from $\mathcal{N}_2\left(\mathbf{0}_2, \begin{pmatrix} 1 & -0.75 \\ -0.75 & 1 \end{pmatrix}\right)$ and $\mathcal{E}_3\left(\begin{pmatrix} 1 \\ 0.5 \\ 0.25 \end{pmatrix}\right)$. We constructed $(0.95, 0.90)$ hyperrectangular tolerance regions for the bivariate normal distribution and $(0.95, 0.90)$ upper semi-space tolerance regions for the trivariate exponential distribution. For our coverage study, we used $B_1 = B_2 = 500$ bootstrap samples for the two layers of the bootstrap calibration and repeated

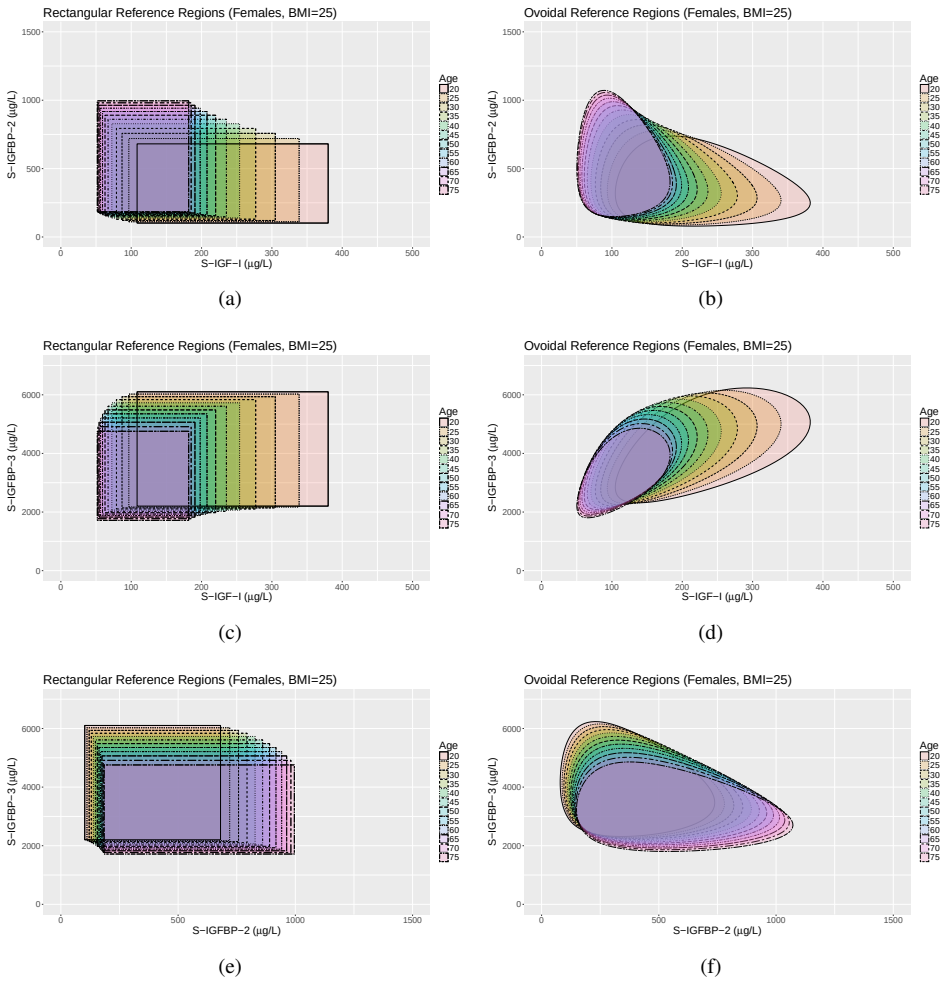

Figure 10. Pairwise plots of reference regions using 0.95-expectation hyperrectangular tolerance regions ((a),(c), and (e)) and 95% normal-based confidence regions in ((b), (d), and (f)). These reference regions are for healthy females by age at a fixed BMI of 25 kg/m^2.

the procedure $M = 1000$ times. The results are reported in Table 19 along with the coverage results when using our nonparametric procedure. The bootstrap calibration has clearly improved the conservative coverage probabilities obtained in the uncalibrated setting. These preliminary results for using a bootstrap calibration when constructing parametric hyperrectangular tolerance regions are promising. However, there is a considerable computational expense for this procedure, which will be a challenging component of this future research.

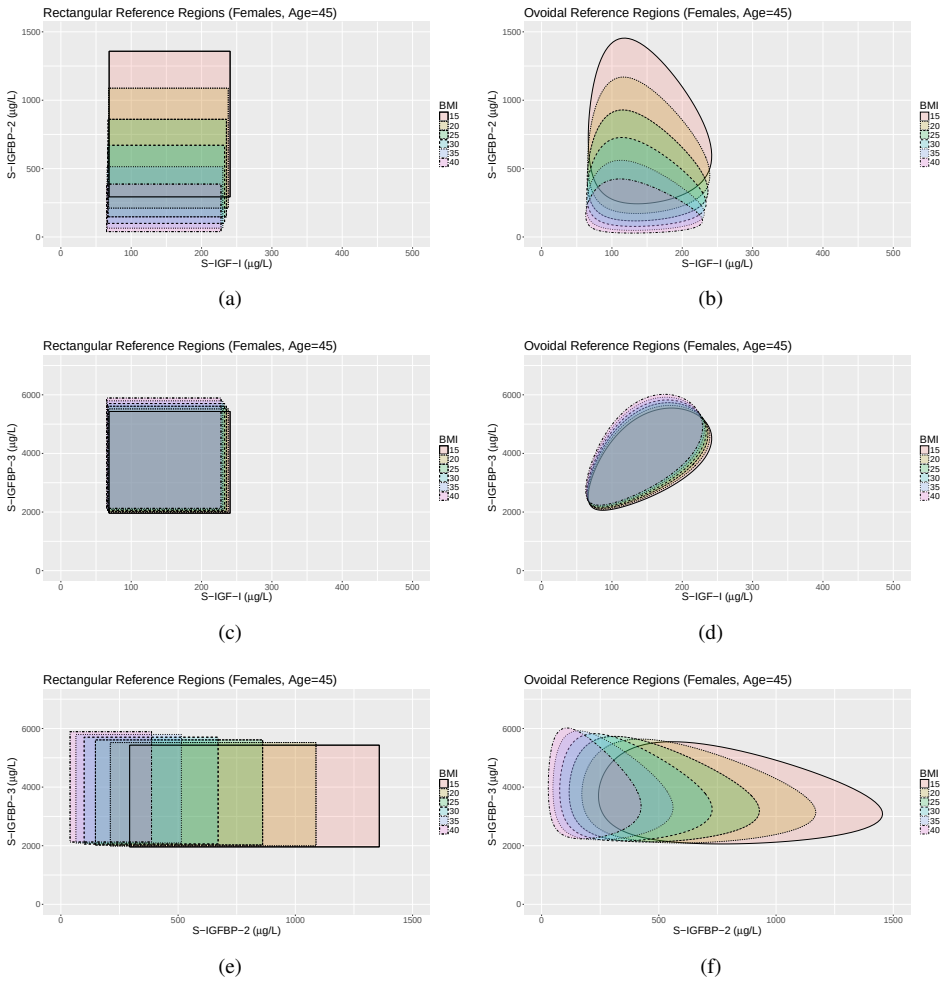

Figure 11. Pairwise plots of reference regions using 0.95-expectation hyperrectangular tolerance regions ((a),(c), and (e)) and 95% normal-based confidence regions in ((b), (d), and (f)). These reference regions are for healthy females by BMI at a fixed age of 45 years.

References

1. Ichihara K and Boyd JC. An appraisal of statistical procedures used in derivation of reference intervals. *Clinical Chemistry and Laboratory Medicine* 2010; 48(11): 1537–1551.
2. Boyd JC and Lacher DA. The multivariate reference range: An alternative interpretation of multi-test profiles. *Clinical Chemistry* 1982; 28(2): 259–265.

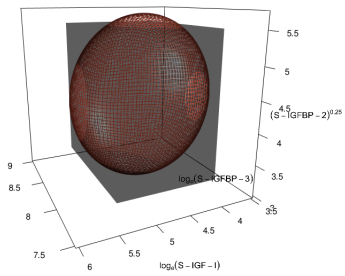

Figure 12. Full trivariate reference regions plotted on the transformed scales of the responses for males 45 years of age with a BMI of 25 kg/m^2. Both the $(0.95, 0.95)$ hyperrectangular tolerance region and 95% normal-based confidence region are shown.

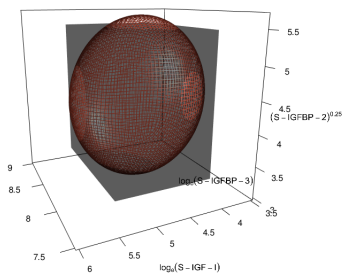

Figure 13. Full trivariate reference regions plotted on the transformed scales of the responses for females 45 years of age with a BMI of 25 kg/m^2. Both the $(0.95, 0.95)$ hyperrectangular tolerance region and 95% normal-based confidence region are shown.

3. Krishnamoorthy K and Mathew T. *Statistical Tolerance Regions: Theory, Applications, and Computation*. Hoboken, NJ: Wiley, 2009.
4. Liu RY. On a notion of data depth based on random simplices. *The Annals of Statistics* 1990; 18(1): 405–414.
5. Zuo Y and Serfling R. General notions of statistical depth functions. *The Annals of Statistics* 2000; 28(2): 461–482.

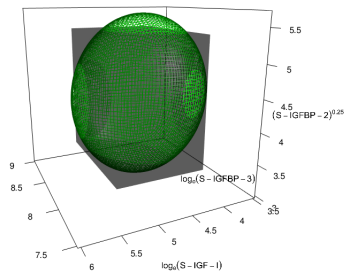

Figure 14. Full trivariate reference regions plotted on the transformed scales of the responses for males 45 years of age with a BMI of 25 kg/m^2. Both the 0.95-expectation hyperrectangular tolerance region and 95% normal-based confidence region are shown.

Table 19. Coverage study results for the parametric bootstrap calibration. Nominal coverage level is 0.90.

Distribution	n	**Uncalibrated**	**Calibrated**	**Nonparametric**
Bivariate	50	0.976	0.872	0.363
Normal	150	0.992	0.913	0.967
Trivariate	50	0.996	0.913	0.470
Exponential	150	0.998	0.880	0.938

6. Serfling R. Depth functions in nonparametric multivariate inference. In Liu RY, Serfling R and Souvaine DL (eds.) *DIMACS Series in Discrete Mathematics and Theoretical Computer Science - Data Depth: Robust Multivariate Analysis, Computational Geometry and Applications*, volume 72. Rhode Island, USA: The American Mathematical Society, 2006. pp. 1–16.
7. Mahalanobis PC. On the generalized distance in statistics. *Proceedings of the National Academy of Sciences, India* 1936; 2(1): 49–55.
8. Tukey JW. Mathematics and the picturing of data. In *Proceedings of the International Congress of Mathematicians, Vancouver 1974*, volume 2. USA: Canadian Mathematical Congress, 1975. pp. 523–532.
9. Donoho DL and Gasko M. Breakdown properties of location estimates based on halfspace depth and projected outlyingness. *The Annals of Statistics* 1992; 20(4): 1803–1827.
10. Oja H. Descriptive statistics for multivariate distributions. *Statistics and Probability Letters* 1983; 1(6): 327–332.
11. Vardi Y and Zhang CH. The multivariate l_1-median and associated depth. *Proceedings of the National Academy of Sciences* 2000; 97(4): 1423–1426.
12. Serfling R. A depth function and a scale curve based on spatial quantiles. In Dodge Y (ed.) *Statistical Data Analysis Based On the L_1-Norm and Related Methods*. Basel, Switzerland: Birkhaüser Verlag, 2002. pp. 25–38.

13. Chaudhuri P. On a geometric notion of quantiles for multivariate data. *Journal of the American Statistical Association* 1996; 91(434): 862–872.
14. Dyckerhoff R, Mosler K and Koshevoy G. Zonoid data depth: Theory and computation. In Pratt A (ed.) *COMPSTAT 1996: Proceedings in Computational Statistics*. Heidelberg: Physica-Verlag, 1996. pp. 235–240.
15. Mosler K and Hoberg R. Data analysis and classification with the zonoid depth. In Liu RY, Serfling R and Souvaine DL (eds.) *DIMACS Series in Discrete Mathematics and Theoretical Computer Science - Data Depth: Robust Multivariate Analysis, Computational Geometry and Applications*, volume 72. Rhode Island, USA: The American Mathematical Society, 2006. pp. 49–59.
16. Liu X and Zuo Y. Computing projection depth and its associated estimators. *Statistics and Computing* 2014; 24(1): 51–63.
17. Elmore RT, Hettmansperger TP and Xuan F. Spherical data depth and a multivariate median. In Liu RY, Serfling R and Souvaine DL (eds.) *DIMACS Series in Discrete Mathematics and Theoretical Computer Science - Data Depth: Robust Multivariate Analysis, Computational Geometry and Applications*, volume 72. Rhode Island, USA: The American Mathematical Society, 2006. pp. 87–101.
18. Tyler DE. A distribution-free M-estimator of multivariate scatter. *The Annals of Statistics* 1987; 15(1): 234–251.
19. Rousseeuw PJ and Ruts I. Bivariate location depth. *Journal of the Royal Statistical Society, Series C (Applied Statistics)* 1996; 45(4): 516–526.
20. Aloupis G and McLeish E. A lower bound for computing Oja depth. *Information Processing Letters* 2005; 96(4): 151–153.
21. R Core Team. *R: A Language and Environment for Statistical Computing*. R Foundation for Statistical Computing, Vienna, Austria, 2015. URL https://www.R-project.org/.
22. Benaglia T, Chauveau D, Hunter DR et al. mixtools: An R package for analyzing finite mixture models. *Journal of Statistical Software* 2009; 32(6): 1–29. Http://www.jstatsoft.org/v32/i06/.
23. Pokotylo O, Mozharovskyi P and Dyckerhoff R. *Depth-Based Classification and Calculation of Data Depth*, 2015. URL http://CRAN.R-project.org/package=ddalpha. R package version 1.1.3.1.
24. Cuesta-Albertos JA and Nieto-Reyes A. The random tukey depth. *Computational Statistics and Data Analysis* 2008; 52(11): 4979–4988.
25. Dovoedo YH and Chakraborti S. Power of depth-based nonparametric tests for multivariate locations. *Journal of Statistical Computation and Simulation* 2015; 85(10): 1987–2006.
26. Dang X and Serfling R. Nonparametric depth-based multivariate outlier identifiers, and masking robustness properties. *Journal of Statistical Planning and Inference* 2010; 140(1): 198–213.
27. Serfling R and Wijesuriya U. Depth-based nonparametric description of functional data, with emphasis on use of spatial depth. *Computational Statistics and Data Analysis* 2017; 105: 24–45.
28. Young DS and Mathew T. Improved nonparametric tolerance intervals based on interpolated and extrapolated order statistics. *Journal of Nonparametric Statistics* 2014; 26(3): 415–432.
29. Brown LD, Cai TT and DasGupta A. Interval estimation for a binomial proportion. *Statistical Science* 2001; 16(2): 101–133.
30. Mattsson A, Svensson D, Schuett B et al. Multidimensional reference regions for igf-i, igfbp-2 and igfbp-3 concentrations in serum of healthy adults. *Growth Hormone & IGF Research* 2008; 18(6): 506–516.
31. Efron B and Tibshirani RJ. *An Introduction to the Bootstrap*. London: Chapman & Hall/CRC, 1993.